

QUASI-PHASEMATCHED NONLINEAR INTERACTIONS AND DEVICES

ROBERT L. BYER

*Department of Applied Physics,
Center for Nonlinear Optical Materials,
Stanford University, Stanford, CA 94305, USA*

Received 20 April 1997

The field of nonlinear optics began nearly simultaneously in the United States and in Russia in 1962. The early years of discovery led to an understanding of nonlinearity in materials, phasematching, and nonlinear device performance. In the second decade of the 1970s, tunable parametric oscillators driven by high-peak-power Q-switched lasers made the transition to tools useful for spectroscopy and remote sensing. In the late 1980s engineered nonlinear materials were introduced with the successful implementation of quasi-phasematching by periodic inversion of ferroelectric domains in lithium niobate. Lithographic processing techniques enabled the fabrication of quasi-phasematched nonlinear "chips" using electric field poling of lithium niobate at the wafer scale.

1. Historical Perspective

The early progress in nonlinear optics has been the subject of numerous monographs, review papers and texts. It will suffice for this introduction to direct the reader to the monograph by Bloembergen,¹ and to the book by Akhmanov and Khokhlov.² Harris³ reviewed the progress in parametric oscillators in 1969 following the first experimental demonstration of second harmonic generation in KDP by Franken *et al.*⁴ and the early experimental success in nonlinear interactions.

Efficient nonlinear interactions require, in addition to a nonlinear response in the medium, a means of achieving phase velocity matching of the interacting waves over an interaction distance of many optical wavelengths. Two methods of achieving phasematching and thus, higher conversion efficiency were the use of crystal birefringence to offset dispersion⁵ and the use of a periodic modulation of the sign of the nonlinear coefficient to reset the optical phase.⁶ This latter approach, suggested by Armstrong *et al.*⁶ is now referred to as quasi-phasematching (QPM).

The idea of parametric amplification and generation of tunable light was proposed and analyzed by Armstrong *et al.*⁶, Kingston⁷, Kroll⁸ and by Akhmanov and Khokhlov⁹ in 1962. Three years later, in 1965, the first experimental demonstration

of a parametric oscillator was achieved by Giordmaine and Miller.¹⁰ They used a *Q*-switched Nd:CaWO₄ laser, frequency doubled to the green in LiNbO₃, to pump a monolithic LiNbO₃ tunable parametric oscillator. Shortly thereafter, the first parametric oscillator was demonstrated in Russia at Moscow State University by S. A. Akhmanov *et al.*¹¹ The Russian parametric oscillator, based on the nonlinear crystal KDP with a tuning range that extended from 957.5 to 1177.5 nm, was pumped by a *Q*-switched frequency doubled Nd:Glass laser. The work on parametric oscillators at Moscow State University was summarized in an article published in 1968.¹²

In 1966, Boyd and Askin¹³ suggested that continuous wave parametric oscillation might be possible in the crystal LiNbO₃. Two years later, in 1968, the first cw, visible, parametric oscillator was demonstrated at Stanford in the group led by






<u>PARAMETRIC FLUORESCENCE IN LiNbO₃</u>		
	<u>TEMPERATURE</u>	<u>CENTER WAVELENGTH</u>
	350°C	5520 Å
	300°C	5700 Å
	250°C	5880 Å
	200°C	6100 Å
	150°C	6330 Å

Fig. 1. Parametric Fluorescence in LiNbO₃. The center wavelength is tuned with crystal temperature. The wavelength varies with radius according to the phasematching conditions. [after Byer and Harris, *Phys. Rev.* **168**, 1064 (1968)]

Professor S. E. Harris. The cw LiNbO_3 Optical Parametric Oscillator (OPO) was pumped by the 514 nm output from an argon ion laser.¹⁴ In a joint experiment with a visiting scientist from Moscow State University, Dr. A. Kovrigin, the work was extended to demonstrate an efficient cw ring cavity parametric oscillator.¹⁵ Dr. Kovrigin's visit to Stanford University followed in the footsteps of his advisor and the founding director of the Moscow State University research program in nonlinear optics, Dr. Rem V. Khokhlov. Professor Khokhlov had visited Stanford ten years earlier in 1959 as a guest of Professor H. Heffner. During his stay at Stanford, Professor Khokhlov was introduced to Professor of history, Richard W. Lyman. In slightly more than one decade following their meeting at Stanford, Professor Khokhlov and his friend Professor Lyman would become the Rector and the President of their respective Universities.

Parametric amplifiers, like all linear amplifiers, have inherent quantum noise.¹⁶ It was realized at Stanford by Harris¹⁷ and almost simultaneously at Cornell by Tang,¹⁸ at Bell Labs by Kleinman,¹⁹ and in Moscow by Klyshko,²⁰ that the parametric noise was intense enough to be visible as fluorescence. Further, this visible fluorescence could be tuned by altering the phasematching conditions of the parametric interaction. A set of striking color photographs of visible parametric fluorescence was published in an article prepared by J. Giordmaine in 1969.²¹ Figure 1 shows the parametric fluorescence emitted by a crystal of LiNbO_3 pumped by an argon ion laser. The center wavelength is tuned by changing the crystal birefringence with temperature. Today, photon "fission" as it was called by Klyshko, is the basis for the generation of correlated paired photons useful for the production of squeezed states of light and for the study of quantum optics.

The research at Stanford led to the first commercial tunable laser source based on a Q-switched, frequency-doubled Nd:YAG laser pumped LiNbO_3 parametric oscillator. The parametric oscillator, introduced by Chromatix in 1971, tuned from less than 550 nm to greater than 4.8 μm when pumped by the 659 nm, 561 nm, 532 nm, and 473.5 nm outputs of a frequency doubled Nd:YAG source. More than 50 of these tunable parametric oscillators were sold worldwide. Figure 2a shows a photograph taken in 1971 of the red tunable output from this parametric oscillator. Figure 2b shows the tuning range of the LiNbO_3 parametric oscillator. A few these devices are still in operation today more than twenty five years after their introduction.

Early progress in nonlinear optics was held back by the lack of useful nonlinear crystals. Research to discover new nonlinear materials progressed slowly, limited by the difficulty in finding crystals with adequate birefringence to achieve phasematching. One study discovered that of 22,000 crystals surveyed, fewer than 100 had adequate birefringence for phasematching. Of these, only a handful could be grown and prepared for characterization of their nonlinear optical properties. Nevertheless, work in Europe and the United States led to the discovery of new classes of nonlinear materials including LiIO_3 , the semiconductors CdSe and proustite, and

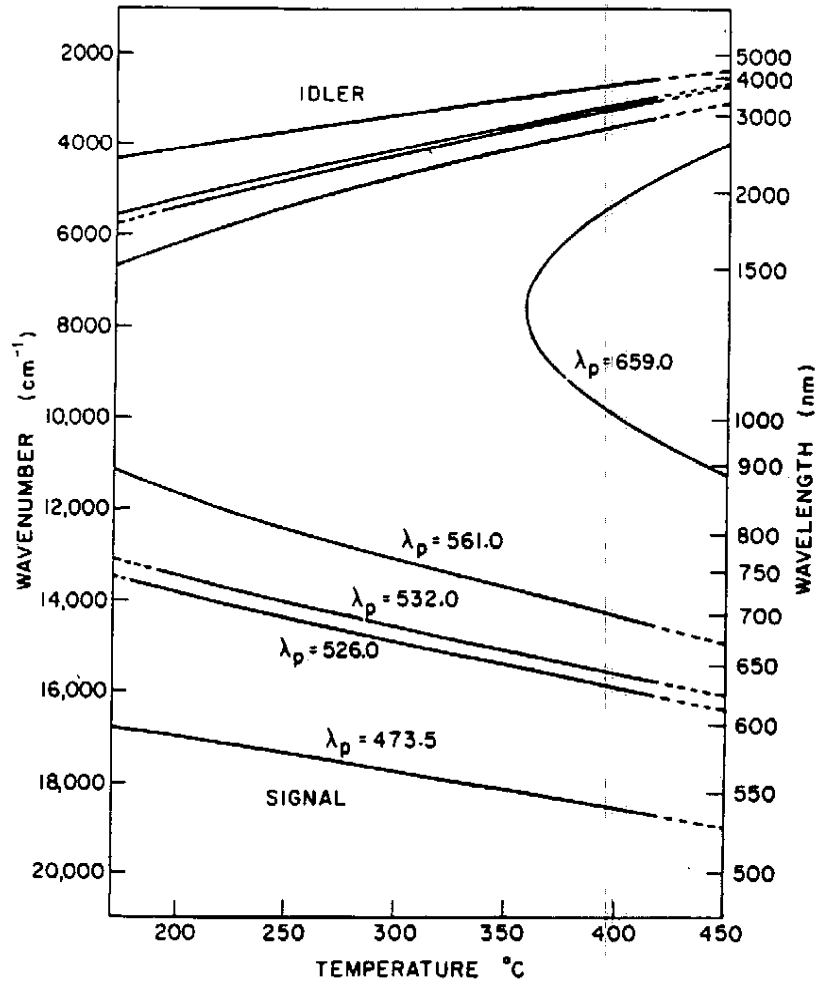
the chalcopyrites AgGaS_2 , AgGaSe_2 , ZnGeP_2 and CdGeAs_2 . Progress in nonlinear materials and devices was reviewed by Byer in 1973.²²

The difficulty in discovering and developing new nonlinear crystals led researchers to revisit the idea first suggested by Bloembergen⁶ that phasematching might be achieved by periodically altering the sign of the nonlinear coefficient (quasi-phasematching). In 1968 Bloembergen took the steps to apply for and to receive a patent on the idea of quasi-phasematching.²³ We will see below that twenty years would pass before quasi-phasematching could be implemented in a practical way.



(a)

Fig. 2. (a) Photograph of the first commercial tunable laser source based on a Q-switched, frequency doubled, Nd:YAG laser pumped LiNbO_3 parametric oscillator introduced in 1971.

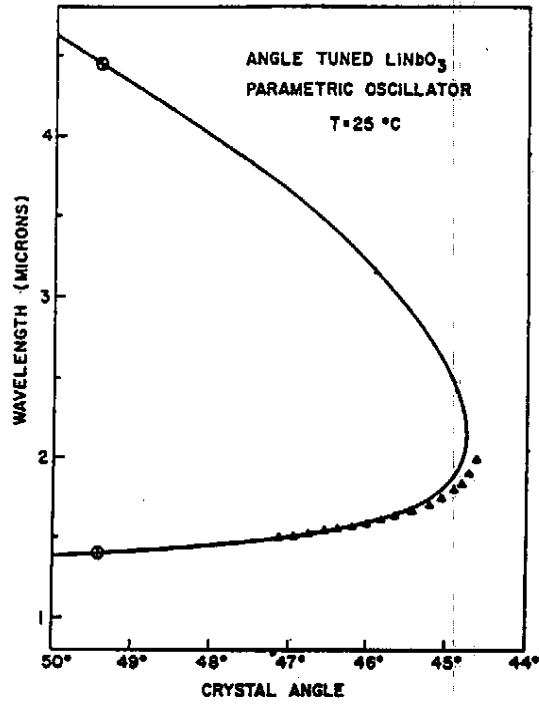


(b)

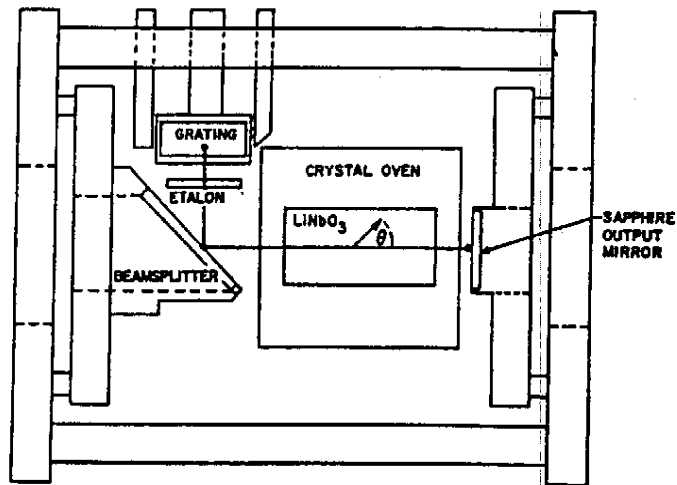
Fig. 2. (b) Wavelength tuning range with temperature of the parametric oscillator when pumped by harmonics of the Nd:YAG laser. [after Byer Ref. 25]

2. High Peak Power Parametric Oscillators and Applications

Although some efforts were applied to finding a practical approach to achieve quasi-phase-matching, progress in the second decade of nonlinear optics was in the area of high peak power nonlinear interactions based on birefringent phase-matching. The key to progress was the combination of improved nonlinear optical materials coupled with improved laser sources. Research took place in many laboratories around the world. I will summarize briefly the progress in tunable parametric oscillators at Stanford and demonstrate their capabilities through descriptions of applications to remote sensing and to Coherent Antistokes Raman Spectroscopy (CARS).



(a)



(b)

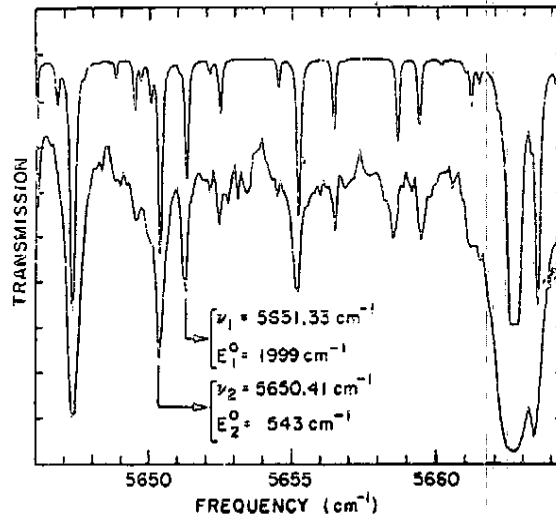
Fig. 3. (a) The 1.4 to 4.4 μm infrared tuning range of the Nd:YAG pumped high-peak-power LiNbO_3 parametric oscillator. (b) Schematic of the parametric oscillator cavity showing the grating and etalon linewidth control elements. The 5 cm long LiNbO_3 crystal is mounted in the crystal oven. The output is to the right through the sapphire output mirror. [after Byer Ref. 33]

Remote sensing of molecular species in the atmosphere was reviewed by Kildal and Byer in 1971.²⁴ The requirements for wavelength tunability with linewidth control, especially in the near infrared molecular fingerprint spectral region, led the Stanford group to develop a high peak power tunable parametric laser transmitter for remote atmospheric sensing.²⁵ The research effort led in turn to the successful demonstration of the unstable resonator Nd:YAG laser oscillator-amplifier that operated *Q*-switched at up to 1 J per pulse at 10 Hz repetition rate.²⁶ This high-peak-power, near-diffraction-limited laser became the pump for a parametric oscillator²⁷ followed by a parametric amplifier.²⁸ The breakthrough in nonlinear crystal technology was the growth of LiNbO₃ along the [014] crystalline axis which led to 1.5 cm diameter by 5 cm long nonlinear crystals²⁹ oriented in the phase-matching direction. With the addition of linewidth control using an intracavity grating in combination with a tilted etalon, the singly resonant parametric oscillator operated in a narrow bandwidth and even in a single axial mode which was required for remote detection of molecular species. Further, the addition of a PDP-11 minicomputer allowed automated tuning of the parametric oscillator over the spectral range from 1.4 to 4.4 μm . Figure 3a shows the 1.4 to 4.4 μm tuning range of the LiNbO₃ parametric oscillator and Fig. 3b shows a schematic of the LiNbO₃ parametric oscillator resonator with computer controlled etalon and a grating for linewidth reduction.

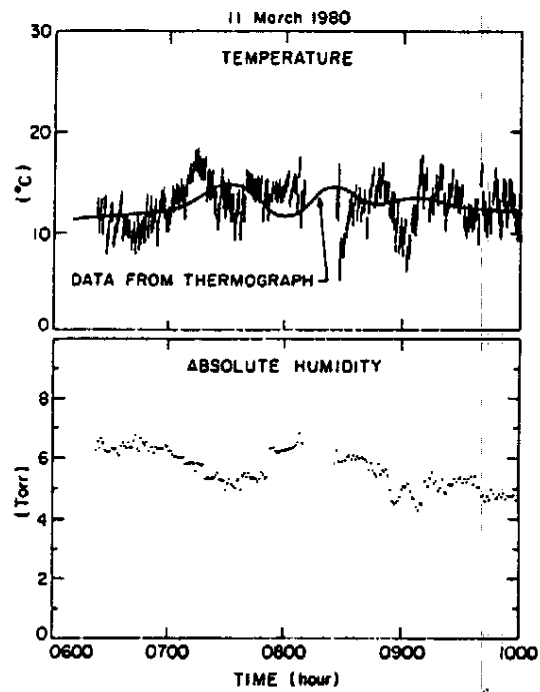
The Nd:YAG laser-pumped computer-tuned parametric oscillator was applied to remote sensing of atmosphere including the detection of SO₂,³⁰ and CH₄.³¹ Improvements in the tunable source led to simultaneous measurements of atmospheric temperature and humidity using on-off tuning between two levels in H₂O vapor with split ground state levels.³² Figure 4a shows the atmospheric absorption spectrum of water vapor over a 775 m path in the 1700 nm region. Figure 4b shows the Lidar measurement of atmospheric temperature and humidity over a four hour period demonstrating the reliability of this first computer tuned parametric oscillator.

Research in the application of the unstable-resonator-pumped computer-controlled LiNbO₃ parametric oscillator was summarized and reviewed by Byer.³³ The work led to the commercialization of the unstable resonator Nd:YAG laser by Quanta Ray in 1976. The high peak power Nd:YAG laser oscillator-amplifier was converted to higher harmonics in KDP and was used to pump a tunable dye laser. The modern version of this laser continues to be used today for pumping parametric oscillators.

The availability of tunable coherent radiation led to a research program to study four wave mixing as a new form of spectroscopy for probing Raman active transitions in molecules. Called Coherent Antistokes Raman Spectroscopy or CARS spectroscopy in the United States,³⁴ it was adopted as a useful approach for exploring Raman spectra at high resolution³⁵ and under extreme conditions such as supersonic expansions.³⁶ Again the research at Stanford was conducted jointly with visitors from Moscow. Dr. Lev Kulevskii visited the Stanford group in 1976 to explore high resolution cw CARS spectroscopy of methane and of molecular

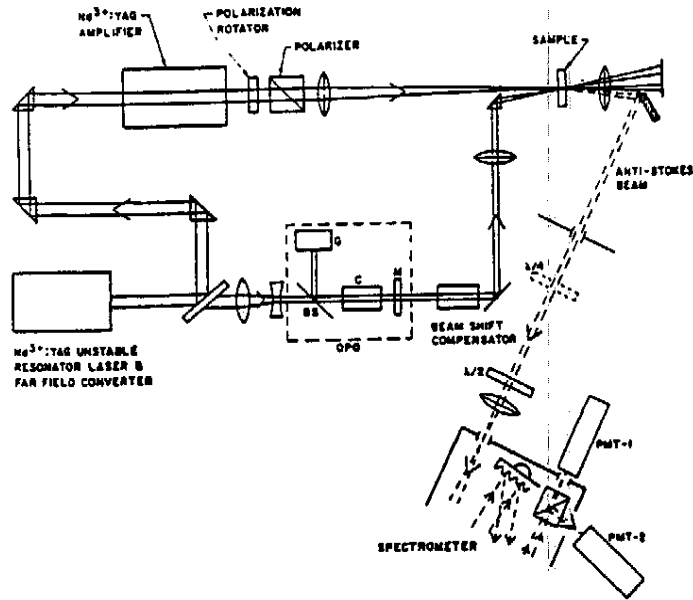


(a)

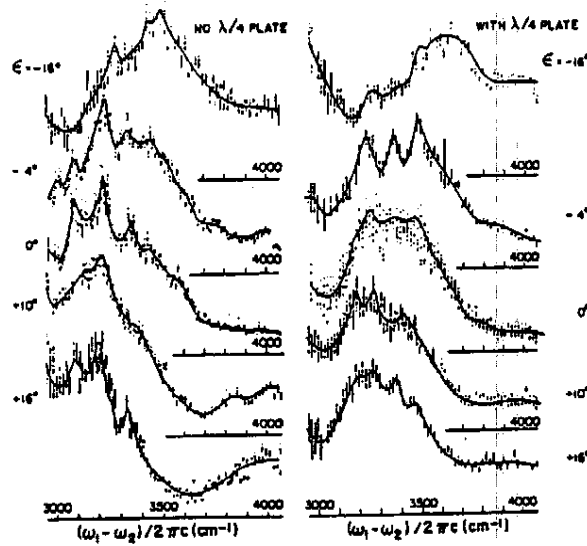


(b)

Fig. 4. (a) Computer controlled LiNbO₃ parametric oscillator spectrum of water vapor absorption lines taken over a 775 m atmosphere path. The OPO linewidth was 0.1 cm⁻¹. (b) Lidar measurement of atmospheric temperature and absolute humidity over a four hour period. [see Ref. 32 for details]



(a)



(b)

Fig. 5. (a) Schematic of the apparatus for polarization CARS spectroscopy of liquid water. The tunable source is a Nd:YAG pumped LiNbO_3 computer tuned OPO. (b) Polarization CARS spectra of liquid water with ϵ the relative polarization angle as a parameter taken with, and without, a quarter wave plate showing structure within the Raman band of liquid water. [after Ref. 38]

hydrogen and its isotopes.³⁷ Two years later, Dr. Nikolai Koroteev visited Stanford and utilized the tunable parametric source to explore the spectra of liquid water using polarization CARS spectroscopy.³⁸ Figure 5a shows the schematic of the polarization CARS experiment. Figure 5b shows the polarization CARS spectra of liquid water. Professor N. Koroteev recently served as the Vice Rector of Moscow State University and is presently the director of the International Laser Center at Moscow State University.

The scientific collaborations with scientists from Russia were facilitated by the Vavilov conference on nonlinear optics held at the Akademgorodok in Novosibirsk, Russia in 1976. That conference on nonlinear optics was attended by many of the founders of field in Russia including R. V. Khokhlov, S. A. Akhmanov, A. I. Kovrigin, D. N. Klyshko, and A. S. Piskarskas. As was tradition, all participated in the Asian-Russia vs European-Russia football (soccer) match including Rem Khokhlov. The author refereed the game.

The research in high-peak-power parametric lasers took a major step forward with the development of beta barium borate crystals (BBO) in 1985 by Chen.³⁹ Chen visited Stanford in 1986 and brought with him BBO crystals for testing. That led to the demonstration of efficient harmonic conversion and to the first BBO optical parametric oscillators pumped by the second and third harmonics of the unstable resonator *Q*-switched Nd:YAG laser.⁴⁰ Research at Cornell University by Professor Tang and his group led to early advances in BBO parametric devices and to improvements in the material properties. Progress in parametric oscillators was reviewed by Tang *et al.* in 1992.⁴¹ Improvements in the growth and the optical quality BBO led to the re-introduction of a commercial tunable parametric oscillator product by Spectra Physics in 1993. Continued progress in the frequency control of the BBO OPO by injection seeding led to the application of these, all-solid-state tunable sources, to spectroscopy including CARS spectroscopy.⁴² Today, BBO parametric oscillators with their broad 0.41 to 2.5 μm tuning range have virtually replaced high peak power dye lasers as the preferred tunable coherent source.

3. High Coherence Continuous Wave Parametric Oscillators

The introduction of laser-diode-pumped Nd:YAG solid state laser in 1985⁴³ led to the invention and demonstration of a single frequency monolithic laser diode-pumped ring Nd:YAG laser oscillator⁴⁴ with an oscillation linewidth of less than 10 kHz. This highly coherent laser opened the door to experiments in continuous wave nonlinear frequency conversion by resonance enhancement, including intracavity⁴⁵ and externally resonant second harmonic generation.⁴⁶ For example, a 40 mW single frequency nonplanar ring Nd:YAG laser was converted to 20 mW of 532 nm output in a monolithic resonant ring frequency doubler using MgO:LiNbO₃. The 20 mW, 532 nm second harmonic output then pumped a cw doubly-resonant (DR-) OPO to yield 8 mW of tunable near infrared radiation.⁴⁷ Figure 6a shows a schematic of the monolithic ring cavity MgO:LiNbO₃ OPO that utilized one total

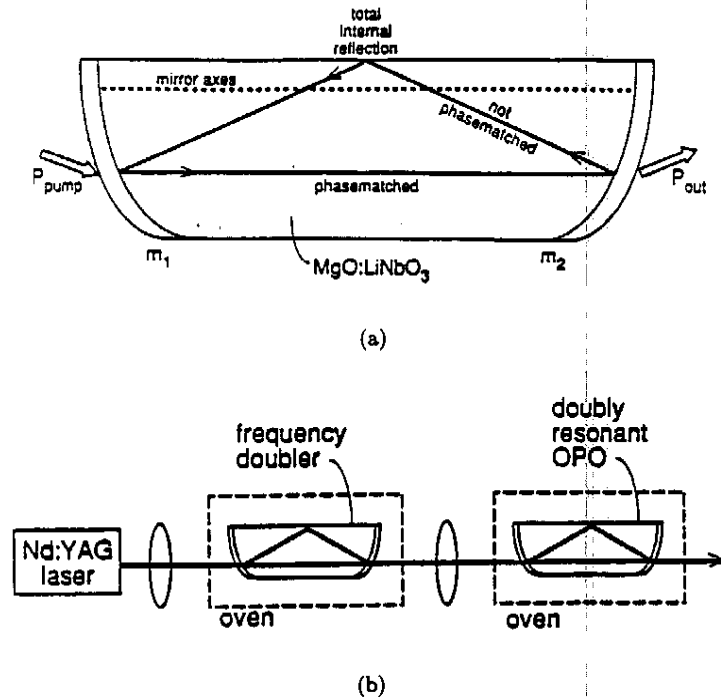


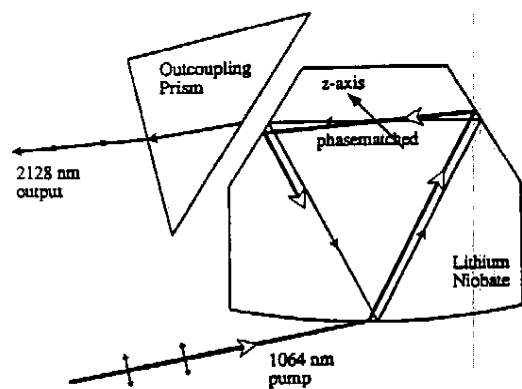
Fig. 6. (a) Schematic of a monolithic doubly-resonant optical parametric oscillator based on MgO:LiNbO₃. The DRO is pumped at 532 nm and oscillates in the 1000 to 1140 nm region in a single axial mode at the signal and idler wavelengths. (b) Schematic of the monolithic ring frequency-doubler and doubly-resonant OPO based on MgO:LiNbO₃. 40 mW of incident 1064 nm from the Nd:YAG laser was converted to 20 mW of 532 nm which pumped the cw DRO and generated 8 mW of single axial mode tunable output. [after Ref. 48]

internal reflection bounce. Figure 6b shows the diode pumped Nd:YAG single frequency laser, the monolithic frequency doubler and the monolithic ring resonator MgO:LiNbO₃ doubly resonant OPO.

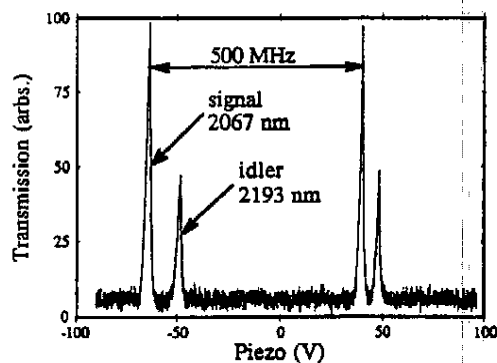
In 1989, Nabors *et al.*⁴⁸ demonstrated a < 20 mW threshold cw monolithic LiNbO₃ OPO with < 13 kHz linewidth and greater than 80% conversion efficiency. This monolithic OPO operated stably and demonstrated phaselocked operation at degeneracy, where the signal and idler frequencies of the OPO locked into a single frequency at exact degeneracy, thus, demonstrating the first frequency divider in the optical region. The tuning characteristics of cw monolithic doubly-resonant oscillator (DRO) were studied in detail by Eckardt *et al.*⁴⁹ Eckardt *et al.* also remeasured the nonlinear optical coefficients of many crystals, setting a modern standard for nonlinear coefficient values.⁵⁰

The design and demonstration of total internal reflection (TIR) parametric oscillators was motivated by the desire for very low threshold devices and for broad tunability without the limitations of bandwidth imposed by dielectric mirror coatings. Schiller⁵¹ designed and demonstrated a 1064 nm cw pumped quadruply-resonant OPO with a threshold of 0.4 mW. This device was pumped at the sumharmonic,

1064 nm, which through TIR resonance led to efficient production of 532 nm. The resonant 532 nm in turn, pumped a TIR OPO which oscillated with doubly-resonant at the signal and idler waves near degeneracy. Dubbed the monolithic total-internal-reflection resonator or MOTIRR, this device illustrated that low loss, stability, and high conversion efficiency could be achieved in TIR structures. In similar work Serkland *et al.*⁵² demonstrated a TIR-cw-pumped OPO based on angle phasematching in LiNbO_3 . The output waves at 2040 and 2225 nm were resonant with a finesse within the LiNbO_3 TIR cavity of greater than 6000. The low loss led to a cw threshold of 130 mW despite the interaction length limitations due to Poynting vector walk-off in the angle phasematched crystal. The monolithic nature of the device led to single mode oscillation recorded for more than 20 minutes without



(a)



(b)

Fig. 7. (a) A Schematic of a total-internal-reflection (TIR) optical parametric oscillator pumped by a cw 1064 nm Nd:YAG laser. The signal and idler resonator losses are less than 0.1% round trip leading to a pump threshold of 130 mW. (b) OPO output at the signal and idler waves. The output was stable for 30 minutes on a single axial mode of the signal and idler waves. [after Ref. 52]

feedback control. Figure 7a shows the schematic of the monolithic LiNbO₃ OPO pumped by a cw 1064 nm laser source. Figure 7b shows the single axial mode pair at the signal and idler wave outputs at 2067 and 2193 nm, respectively. A critical feature of this TIR OPO was the use of birefringence to couple the pump light into the resonator.

The third area of progress towards highly coherent continuous wave parametric oscillators was the first successful demonstration of a cw singly-resonant parametric oscillator. The threshold of the singly-resonant OPO is approximately 200x higher than for a doubly-resonant OPO at a comparable loss but the singly-resonant oscillator (SRO) offers ease of continuous tunability without axial mode jumps from the cluster effect first noted by Giordmaine and analyzed in detail for the DRO by Eckardt *et al.*⁴⁹ The high threshold of the SRO led A. Nilsson to write in his thesis that "a nightmarish dissertation might involve using a low power (Nd:YAG) Nonplanar Ring Oscillator to injection lock a high power oscillator that is then resonantly doubled to drive a cw, singly resonant OPO."⁵³ In fact, this experiment was successfully completed using a lamp pumped, 20W cw Nd:YAG laser injection locked to produce 19 W of single axial mode output.⁵⁴ The laser was then frequency doubled in an external resonant cavity using LBO to produce 11 W of cw 532 nm output. The 532 nm was used to pump a KTP singly resonant OPO which operated with a threshold of less than 4 W and generated 1.9 W of cw output with 70% slope efficiency. Further, the SRO operated in a single axial mode at the resonated wave⁵⁵ as predicted more than twenty-five years earlier by Harris.³

The progress in optical parametric oscillation and amplification was the focus in special issues of the Journal of the Optical Society of America B edited by A. Piskarskas of the Laser Research Center, Vilnius University, Lithuania and R. L. Byer of Stanford University.⁵⁶ The articles featured the considerable progress and achievements in parametric devices made during the previous two decades. Progress in continuous wave parametric devices, pulsed high peak power infrared tunable sources, visible parametric sources and spectroscopic applications were covered. A section of the special issue was devoted to synchronously pumped and travelling wave picosecond and femtosecond parametric devices, an area pioneered by Piskarskas, Laubereau and Tang and actively pursued by Hanna, Ferguson, Wallenstein and others.⁵⁶

A second special issue on Optical Parametric Devices, edited by W. R. Bosenberg and R. C. Eckardt, was published in the Journal of the Optical Society of America B, November 1995.⁵⁷ The progress in parametric devices highlighted in that issue included highly efficient devices; frequency control and spectroscopic applications; picosecond and femtosecond synchronously pumped parametric devices; parametric amplifiers, quantum optical effects and squeezing in parametric processes. Also included was a contribution on quasi-phasematched (QPM) optical parametric oscillators in bulk periodically poled LiNbO₃.⁵⁸ Progress in QPM nonlinear optical materials during the preceding five years had allowed QPM parametric oscillator devices to be demonstrated based on domain inversion in ferroelectric LiNbO₃. The

next section introduces quasi-phasematched nonlinear interactions and reviews the early progress in quasi-phasematched materials and devices.

4. Quasi-Phasematched Nonlinear Interactions

If the nonlinear interaction is not phasematched, the energy flows from the fundamental to the harmonic wave for one coherence length then reverses as the interaction is out of phase. If the sign of the nonlinear coefficient is reversed every coherence length, l_c , then the nonlinear interaction continues to grow. Figure 8 illustrates the phasematched interaction using birefringence and the quasi-phasematched interaction for 1st-order quasi-phasematching (QPM). Here the nonlinear material is assumed to be a ferroelectric crystal with spontaneous polarization P_s . Upon reversal of the ferroelectric domain indicated by the arrows in Fig. 8, the sign of the nonlinear coefficient is also reversed. The advantages of QPM are the possibility of phasematching in crystals that are not birefringent but have large nonlinear optical coefficients such as GaAs and ZnSe; the possibility of utilizing the largest nonlinear coefficient for the interaction and thus enhancing the nonlinear gain; and the possibility of purposefully tailoring the spatially modulated nonlinear coefficient to achieve particularly useful interactions. The advantages of quasi-phasematching motivated early workers to continue the search for practical approaches to periodically reversing the sign of the nonlinear coefficient. A brief summary of the early work, and a detailed theoretical treatment of quasi-phasematched interactions is provided by Fejer *et al.*⁵⁹ A review of early progress in quasi-phasematched interactions is presented by Byer.⁶⁰

The theory for quasi-phasematched nonlinear interactions is an extension of the theory developed for birefringently phasematched interactions.⁵⁸ However the

QUASI-PHASEMATCHING

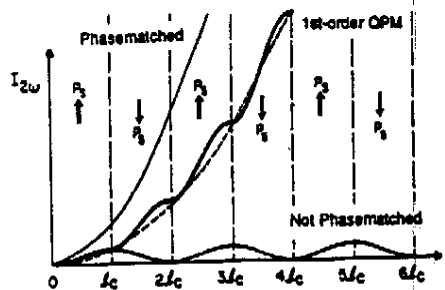


Fig. 8. The second harmonic intensity $I_{2\omega}$ vs propagation distance in the nonlinear crystal in units of the coherence length, l_c . The Phasematched and the 1st-order quasi-phasematched (QPM) interactions are shown. P_s is the spontaneous polarization of the ferroelectric crystal. Inversion of the spontaneous polarization corresponding to inversion of a ferroelectric domain, results in inversion of the sign of the nonlinear optical coefficient.

nonlinear coefficient is described as a periodic modulated function of distance by the Fourier series

$$d(z) = d_{\text{eff}} \sum_{m=-\infty}^{m=\infty} G_m \exp(-ik_m z) \quad (1)$$

where $d(z)$ is the periodically modulated nonlinear coefficient, d_{eff} is the effective nonlinear coefficient for the propagation direction and polarization, and G_m is the Fourier coefficient given by

$$G_m = (2/m\pi) \sin(m\pi D) \quad (2)$$

where $D = l/\Lambda$ is the duty factor of the QPM reversed domain grating with l the length of the reverse domain and Λ the period of reversal. Here $k_m = 2\pi m/\Lambda$ is the grating vector of the m th Fourier component.

For the QPM interaction the effective nonlinear coefficient is

$$d_Q = d_{\text{eff}} G_m \quad (3)$$

and the wavevector mismatch is given by

$$\Delta k_Q = k_p - k_s - k_i - k_m \quad (4)$$

where the indices p , s , and i refer respectively to the interacting pump, signal and idler waves. For three wave nonlinear interactions the frequencies are related by

$$\omega_p = \omega_s + \omega_i. \quad (5)$$

At degeneracy, $2\omega_s = 2\omega_i = \omega_p$ and the pump frequency is the harmonic of the fundamental frequency ω_s . For $m = 1$, or first order QPM interactions, the wavevector mismatch becomes

$$\Delta k_Q = k_p - k_s - k_i - 2\pi/\Lambda \quad (6)$$

where the period Λ is twice the coherence length l_c or

$$\Lambda = 2l_c = 2\pi/(k_p - k_s - k_i) \quad (7)$$

For a domain duty cycle of $D = 50\%$ we find that the nonlinear coefficient for the QPM interaction is given by

$$d_Q = (2/\pi)d_{\text{eff}}. \quad (8)$$

The coupled equations governing the three wave parametric interaction for QPM phasematching are given by⁵⁸

$$\frac{dE_s}{dz} = \frac{i\omega_s}{n_s c} d_Q E_p E_i^* \exp(\Delta k_Q z) \quad (9a)$$

$$\frac{dE_i}{dz} = \frac{i\omega_i}{n_i c} d_Q E_p E_s^* \exp(\Delta k_Q z) \quad (9b)$$

$$\frac{dE_p}{dz} = \frac{i\omega_p}{n_p c} d_Q E_s E_i \exp(-\Delta k_Q z) \quad (9c)$$

In the limit of low gain, the single pass parametric gain from Eq. (9) is given by^{25,58,59}

$$G(L) = \{E_s(L)/E_s(0)\}^2 - 1 \sim \frac{2\omega_s\omega_i d_Q^2}{n_s n_i n_p \epsilon_0 c^3} I_p L^2 \text{sinc}^2(\Delta k_Q L/2) \quad (10)$$

where I_p is the pump intensity and L is the interaction length in the nonlinear crystal. It was noted by Harris (3) that in the low gain limit, the parametric gain and second harmonic conversion efficiency are equal as is expected.

Phasematching is achieved when Δk_Q is zero or

$$\Delta k_Q = k_p - k_s - k_i - 2\pi/\Lambda = 0 \quad (11)$$

assuming a first order interaction. The first three terms of Eq. (11) are the conventional phasematching condition which can be reached by the conventional methods of using birefringence to offset crystal dispersion. The QPM grating vector in Eq. (11) offers the ability to phasematch the interaction by adjusting the QPM grating period. This flexibility coupled with the ability to select the largest nonlinear coefficient for the interaction brings significant advantages to quasi-phasematching.

To gain an appreciation for the scale of Λ consider second harmonic generation. Let λ be the fundamental wavelength, and n_2 and n_1 be the indices of refraction of the medium at the fundamental and generated second harmonic wavelengths. Quasi-phasematching is achieved by changing the sign of the nonlinear coefficient periodically to reset the π phaseshift of the nonlinear interaction after a coherence length defined by $l_c = \lambda/4(n_2 - n_1)$. The coherence length for second harmonic generation from $\lambda = 1 \mu\text{m}$ to the visible is approximately $\lambda/0.1$ or $\sim 10\lambda$. Thus, inversion of the nonlinear coefficient is required approximately every 10 microns which precludes the use of a stack of plates approach to quasi-phasematching. Early work in QPM studied methods of inverting ferroelectric domains in crystals such a LiNbO_3 , LiTaO_3 during crystal growth.

Domain inversion during crystal growth was studied by Feng *et al.*⁶¹ in lithium niobate melts doped with yttrium to enhance periodic inversion of domains at the melt-solid interface. Crystals were grown with periodic domains adequate for second harmonic generation. Later, Feisst and Koidl grew lithium niobate crystals with periodic domains appropriate for nonlinear frequency mixing.⁶² Recently, Aleksandrovskii *et al.*⁶³ have extended the study of periodic domain formation by growing lithium niobate along the pseudocubic (0112) direction to obtain a flat interface. Growth of domain inverted lithium niobate single crystal fibers⁶⁴ was reported by Lu *et al.* in 1986.⁶⁵ This work led to the successful growth of LiNbO_3 single crystal fibers with $3 \mu\text{m}$ spaced domains by Magel⁶⁶ that were used in early frequency doubling experiments to produce blue light.

A significant step in device demonstration was taken by Jundt *et al.*⁶⁷ who used laser-heated pedestal growth⁶⁴ to prepare a $250 \mu\text{m}$ diameter single crystal fiber

of LiNbO_3 , 1.24 mm long, with a domain spacing of $3.47 \mu\text{m}$. The sample was antireflection coated and placed within an external resonant cavity to generate 2 W of cw 532 nm output from a 4 W incident 1064 nm power from a Nd:YAG laser. The circulating power incident on the lithium niobate single crystal fiber was 65 W or $10 \text{ MW}/\text{cm}^2$. The conversion efficiency in this externally resonant second harmonic generation experiment reached 67%. For the first time, QPM lithium niobate had operated in an efficient manner at average power levels in the Watt range.

It became clear in the late 1980's that there were multiple approaches to domain inversion in ferroelectric crystals. Domain inversion by chemical diffusion of titanium into the surface of a heated crystal of LiNbO_3 was suggested by Fejer following the earlier observations in 1979 by Miyazawa,⁶⁸ that titanium diffused into lithium niobate gave rise to domain alteration during waveguide fabrication. Nakamura⁶⁹ used titanium diffusion to fabricate a periodically domain inverted lithium niobate sample for surface acoustic wave devices in 1986. Shortly thereafter, Lim *et al.*⁷⁰ used titanium diffusion to periodically pole lithium niobate for second harmonic generation to yield green and then blue output in 1989. Similar results were obtained almost simultaneously by Webjorn *et al.*⁷¹ Chemical diffusion poling was extended to KTP by Bierlein *et al.*,⁷² and by van der Poel *et al.*⁷³ The diffusion of barium ions into KTP led to domain periods of $4 \mu\text{m}$ which was adequate to phasematch for the generation of 425 nm radiation.

Periodic poling by titanium diffusion uses lithographic patterning to define the periodic titanium metal array deposited on the crystal surface prior to diffusion. The titanium diffusion process leads to well-defined domains located with a few microns of the surface of the crystal and is appropriate for guided wave interactions. The first demonstration of second harmonic generation in quasi-phasematched interactions by Lim *et al.*⁷⁰ utilized guided wave interactions in crystals poled by titanium diffusion, followed by proton diffusion, to define the waveguide. Progress in the preparation of the QPM material and waveguides is described by Lim *et al.*⁷⁴ A review of progress in waveguide QPM materials and devices is presented by Fejer.⁷⁵ In the review, Fejer develops the theory of waveguide QPM devices and summarizes progress in the preparation of QPM waveguide devices in LiNbO_3 , LiTaO_3 and KTP ferroelectrics. A schematic diagram and a photograph of blue generation in a QPM waveguide is illustrated in the review by Fejer on nonlinear optical frequency conversion.⁷⁶

Other methods were found to control domain inversion including the use of pyroelectricity,⁷⁷ and electric fields either applied directly to the sample or by electron beams.⁷⁸ A significant breakthrough in domain inversion and control was demonstrated by H. Ito⁷⁹ who used electron beams to write domains in lithium niobate and lithium tantalate with periods of $7.5 \mu\text{m}$. It was the success by Ito, limited however by the slow writing speed of the electron beam approach, that led Yamada *et al.*⁸⁰ to investigate domain inversion by direct application of an electric field to metal electrodes deposited by lithographic processing onto the surface of the crystal.

Early work by Camlibel in 1969⁸¹ had shown that electric fields could be used to invert ferroelectric domains at 300 kV/cm applied field to lithium niobate and other oxide ferroelectric crystals. However, dielectric breakdown and the lack of domain control prevented progress toward QPM. A series of studies were undertaken in Russia a decade later in 1978 by Evlanova⁸² as reported by Prokorov and Kuz'minov⁸³ on electric field poling of lithium niobate. Again, results were suggestive but domain control was not achieved to the degree required for device demonstration. The successful control of domain inversion via an applied electric field by Yamada *et al.*⁸⁰ re-opened this promising approach to further study.

Interest in quasi-phases-matched interactions accelerated in the early 1990's to include groups in Japan, the United States and Europe. Although domain modulation during crystal growth produced samples adequate for device demonstration, the technique was not suitable to volume production of QPM material. Therefore, a goal of the research programs was to develop a lithography-based patterning process for creating inverted domains with controlled period and duty cycle. A longer range goal was to mass produce at low cost, quasi-phases-matched nonlinear chips that could be engineered to optimize device performance.

Control of domain inversion and duty cycle proved to be much more difficult than expected. However, persistence coupled with an understanding and modelling of the electric field induced domain inversion process led to success in 1994.^{84,85,86}

The steps taken to define an appropriate processing recipe for lithographic patterned electrodes and room temperature electric field poling of LiNbO₃ are described by Myers.^{58,87} Briefly, the wafer of LiNbO₃ is thoroughly cleaned, patterned and coated with metal electrodes on the +z surface to provide electric field contact for poling. The metal electrodes are overcoated with a thin dielectric layer to inhibit growth of the domains between the metal electrodes. The field is applied to the sample using a liquid electrolyte contact to achieve field uniformity. Domain inversion is initiated when the applied electric field exceeds the coercive field of 21 kV/mm for LiNbO₃ at room temperature. The field is applied for up to 1 second duration by a high voltage supply through a current limiting resistor of 100 M. Both the voltage and current are monitored during the poling process. Domain inversion results in a current flow to compensate the time-dependent change in the spontaneous polarization $P_s = 71 \mu\text{C}/\text{cm}^2$ for LiNbO₃. A charge of $Q = 2P_s A$, where A is the area of reverse domains, is delivered to the sample. For a properly configured circuit, the poling current terminates on completion of poling at a domain duty cycle set by the choice of the electrode width to spacing ratio. The domain duty cycle can be controlled by the correct choice of electrode duty cycle and the applied field in excess of the coercive field. It has been experimentally observed that domains can be inverted without dielectric breakdown for properly prepared wafers. To date poling has been accomplished in wafers up to 1 mm thickness.⁸⁸ Domains revert to their original orientation or can be reversed repeatedly if the field is applied for less than 50 msec. However, the inverted domain regions are permanent for fields

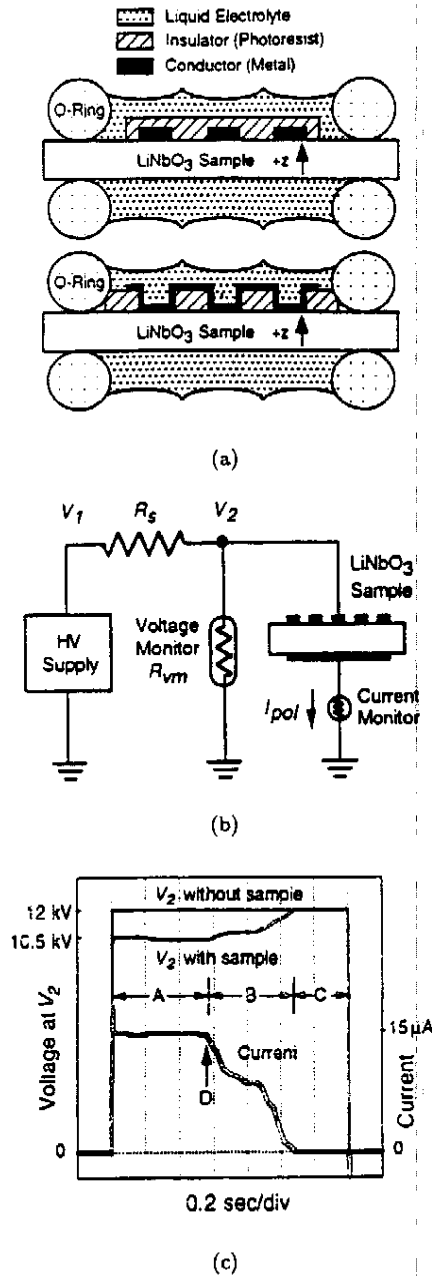
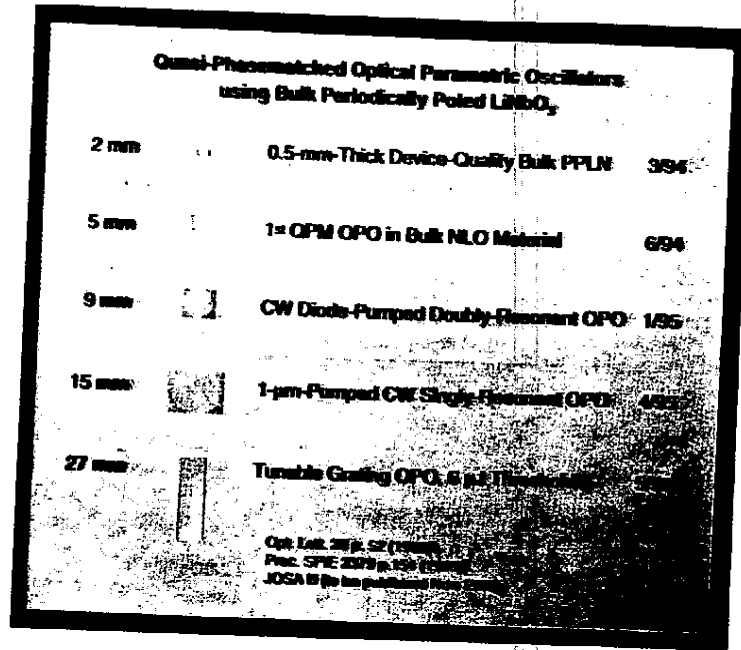
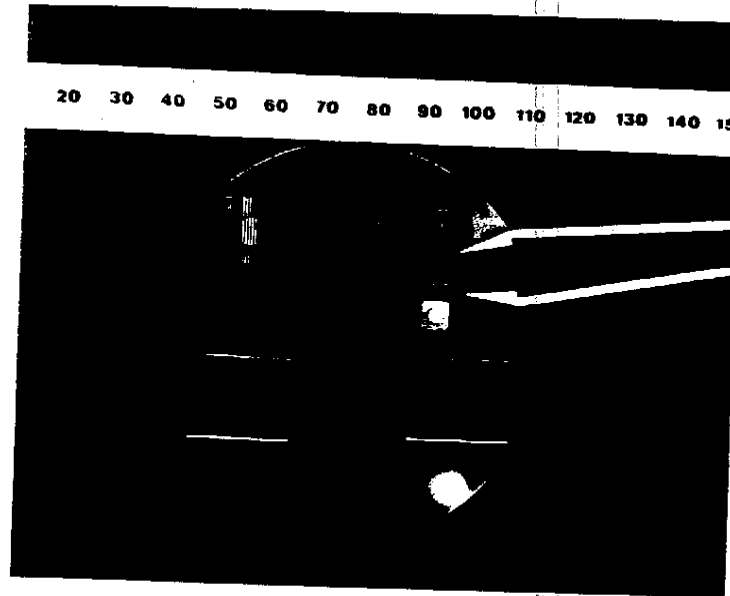


Fig. 9. (a) Schematic of the electrode configuration for electric field poling of a ferroelectric crystal. The ferroelectric domains can be reversed by the application of a sufficient electric field. (b) Electric field poling circuit. Typically $R_s = 100M\Omega$, $R_{vm} = 1G\Omega$, and V_2 is set at 12 kV for a 0.5 mm thick sample of LiNbO₃. During poling V_2 clamps at the coercive voltage V_c . (c) Voltage and current waveforms for poling a 3 mm diameter 0.5 mm thick LiNbO₃ sample. Section A is poling under the metal electrode or liquid contact, Sec. B is poling under the photoresist, and Sec. C is after completion of poling. For a patterned device the voltage would be reduced to zero at point D. [after Ref. 58]



(a)



(b)

Fig. 10. (a) Quasi-phase-matched optical parametric oscillators fabricated using room temperature electric field poling of 0.5 mm thick LiNbO_3 . The bulk devices are described in reference 58. (b) A photograph of a 3 inch diameter wafer of LiNbO_3 on which are assembled for display various OPO device chips.

applied longer than approximately 50 msec after the completion of poling. The domains are made visible by etching with hydrofluoric acid or by observation through crossed polarizers.

Domain periods of 10 to 30 microns suitable for infrared devices were first generated in 2 mm lengths of 0.5 mm thick LiNbO₃ in March, 1994. By May, 1995 the QPM interaction length had been extended to 27 mm. By September of 1995, wafer scale processing of lithium niobate was achieved and nonlinear device "chips" were being fabricated with high yield and reproducible characteristics in 0.5 mm thick by 50 mm long samples based on processing of 3 inch diameter LiNbO₃ wafers.⁸⁷ Figure 10a illustrates the progress in room temperature electric field poling of LiNbO₃. The 27 mm long sample produced in May, 1995 is special in that it contains 25 parametric oscillator QPM gain regions each with a different grating period. Figure 10b shows the photograph of a 3 inch wafer of LiNbO₃ on which are assembled a series of QPM devices for display.

5. Engineered Quasi-Phasematched Nonlinear Devices

5.1. Guided Wave Quasi-Phasematched Nonlinear Devices

The single-pass second harmonic conversion efficiency in bulk nonlinear devices is limited by diffraction spreading of the focussed laser beam. For example, the second harmonic generation (SHG) conversion efficiency for a confocal focussed, 5 cm interaction-length birefringently-phasematched crystal using the d_{31} nonlinear coefficient ($d_{31} = 4.3$ pm/V) in LiNbO₃ is 1.0%/W. A 1 W cw input at 1064 nm yields 10 mW of 532 nm output.

The single pass second harmonic conversion efficiency improves to 17%/W for a 5 cm QPM interaction length with the d_{33} nonlinear coefficient. Here we assume that $d_{33} = 27$ pm/V and that $d_Q = (2/\pi)d_{\text{eff}} = 14.4$ pm/V for the first order QPM interaction. The domain period for this QPM phasematched interaction is $\Lambda = 2l_{\text{coh}} = 6.3$ μm . We will see below that for high power laser sources, the experimentally observed conversion efficiency for cw SHG in bulk QPM interactions is 10%/W. For milliwatt power levels, however, the bulk interaction QPM efficiency remains low and other means must be used to reach high conversion efficiency.

The conversion efficiency can be improved by confining the field to a waveguide. The guided wave interaction allows longer interaction distances at high field intensities by preventing diffraction beam spreading. Fejer⁷⁵ has shown that the conversion efficiency ratio for SHG in a waveguide to that for confocal focussing in bulk is given by

$$\eta(\text{waveguide})/\eta(\text{confocal}) = (L^2/A_{wg})(\lambda_\omega/2\pi_\omega L) = (\lambda_\omega L)/(2\pi_\omega A_{wg}) \quad (12)$$

For a waveguide with an area $A_{wg} = 25$ μm^2 , and an interaction length, $L = 1$ cm, the conversion efficiency for QPM SHG is improved by a factor of 100 to 1000%/W or 1%/mW. Thus, a 20 mW input beam coupled to the waveguide is converted

to the second harmonic, with 20% efficiency, yielding 4 mW at the output of the guided wave QPM device.

For nonlinear interactions in channel waveguides it is customary to characterize the interaction in terms of a normalized conversion efficiency

$$\eta = P_{2\omega}/P_{\omega}^2 = \eta_{\text{nor}}P_{\omega}L^2 \quad (13)$$

where P_{ω} and $P_{2\omega}$ are the measured powers at the fundamental and harmonic waves and L is the interaction length. The normalized conversion efficiency, η_{nor} , is usually expressed in the units of $\%W^{-1}cm^{-2}$. The normalized conversion efficiency is a parameter that is independent of the input coupling into the waveguide. Loss due to input coupling is taken into account by the reduced fundamental power coupled into the waveguide. The normalized conversion factor accounts for the effective nonlinear coefficient, the modal overlap of the interacting fields, and the overlap of the fields with the QPM grating and it is an indicator of the quality of the guided wave QPM interaction.

The first QPM SHG experiment by Lim *et al.*⁷⁰ used a planar waveguide fabricated on the surface of periodically poled LiNbO₃. In that experiment, 1 mW of input was converted to 0.5 nW output at 532 nm. The conversion efficiency was $5\%W^{-1}cm^{-3/2}$ which is in reasonable agreement with the theoretically expected conversion efficiency factor of $7\%W^{-1}cm^{-3/2}$ for the planar waveguide structure.

In a second experiment, the planar waveguide was replaced by a channel waveguide also fabricated on titanium diffused QPM LiNbO₃. The channel waveguide SHG experiment report by Lim *et al.*⁷⁰ doubled an 820 nm tuneable dye laser source to generate 410 nm in a 1 mm long interaction region. The measured normalized conversion efficiency was $37\%W^{-1}cm^{-2}$. The measured normalized conversion efficiency was an order of magnitude below the calculated value due to the triangular shaped depth-dependant QPM domain structure and the consequent reduction in modal overlap.

Improvements in conversion efficiency for SHG in guided wave QPM interactions were achieved in a number of laboratories around the world. In 1992, the normalized conversion efficiency factor of $157\%W^{-1}cm^{-2}$ was achieved in LiTaO₃ by Yamamoto and Mizuuchi⁸⁹ who generated 23 mW of blue light for 121 mW of input power. Roelofs *et al.*⁹⁰ demonstrated $600\%W^{-1}cm^{-2}$ normalized conversion efficiency in KTP. The KTP interaction yielded 9 mW of blue output for 74 mW of input power. Yamada *et al.*⁸⁰ reached $600\%W^{-1}cm^{-2}$ normalized conversion efficiency in electric field poled LiNbO₃. They generated 20.6 mW of blue output for 196 mW of input power.

Although these results were impressive they were yet to be demonstrated in a reproducible manner. In particular, Bortz and Fejer⁹¹ noted that the modal overlap with the triangular shaped QPM domain structure reduced the conversion efficiency. Further, the stringent fabrication tolerances on the waveguide led to scatter losses and modal loss in the waveguide structure. Lim *et al.*⁹² proposed that the waveguide

problem could be solved by using a "non-critical" waveguide design that was less sensitive to fabrication tolerances. For example, a critical waveguide design has an allowable width variation of 2.7 nm, and a non-critical waveguide design has a 27 nm width variation tolerance which is within lithographic fabrication capability for a guide length of 10 mm.

Using the non-critical waveguide design, Bortz *et al.*⁹³ demonstrated a normalized conversion efficiency of $204\%W^{-1}cm^{-2}$ for SHG of 976 nm radiation which is one of the highest values reported for titanium diffused QPM material. The measured normalized efficiency agreed well with that predicted. The modal overlap of the propagating fields in the waveguides and the triangular domains of the diffused titanium QPM structure kept the normalized efficiency from reaching the expected values near $400\%W^{-1}cm^{-2}$ for the TM_{00} mode and $675\%W^{-1}cm^{-2}$ for conversion to the TM_{01} mode. This work placed further emphasis on obtaining QPM domain profiles uniform in depth with 50% duty cycle using poling by electric field in place of titanium diffusion.

Bortz *et al.*⁹⁴ extended their work to the first demonstration of a QPM parametric oscillator and amplifier. The guided wave OPO/OPA operated at single pass gains of 4.1 dB corresponding to $18\%W^{-1}$ gain at a signal wavelength of $1.55\ \mu m$ when pumped by a 782.2 nm source. Parametric oscillation was observed at wavelengths between 1.4 and $1.7\ \mu m$ with a peak output power of 700 mW for an incident peak pump power of 7.7 W coupled into the waveguide.

Figure 11a shows the pulsed parametric oscillator output power and incident pump power vs time. Figure 11b shows the tuning range of the parametric oscillator vs the pump wavelength. This first demonstration of a QPM optical parametric oscillator showed both wavelength generation and parametric gain that could be of significance in the important infrared communications bands.

The QPM waveguide OPO performance has been extended recently by Arbore⁹⁵ who reported a singly-resonant optical parametric oscillator in a QPM guided wave structure. In this case, electric field poling of $LiNbO_3$ was used to fabricate the QPM structure. Parametric gains as high as $250\%/W$ and an oscillation threshold of 1.6 W was measured. Pump depletion of 40% was observed. With further optimization of the waveguide the singly-resonant oscillator is predicted to have a threshold of ~ 100 mW which is accessible to laser diode pumping.

Recent progress in QPM waveguide devices has moved to QPM structures with uniform domain patterns formed by electric-field poling at room temperature,⁸⁰ pyroelectric induced fields,⁷⁷ and focused ion beam writing.⁹⁶ The narrow acceptance bandwidth for blue generation by SHG led to research to control the diode-laser wavelength by Bragg grating feedback combined with QPM phasematched SHG.⁹⁷ In China, Duan Feng and Nai Ben Ming⁹⁸ suggested the use of the aperiodic Fibonacci series to define a superlattice with multiple wavelength conversion and broad spectral acceptance bandwidth to accommodate the laser diode bandwidths for SHG.

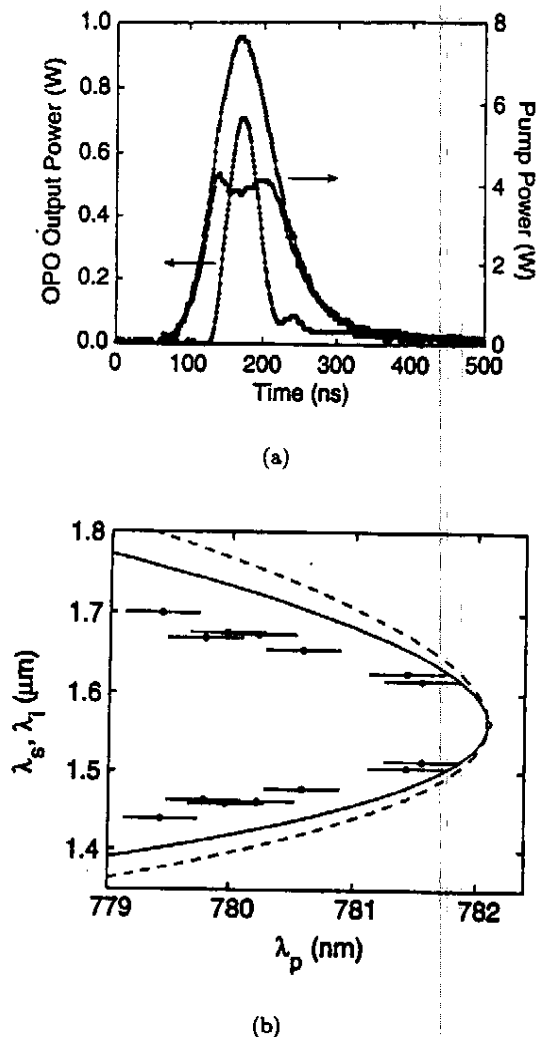


Fig. 11. (a) QPM guided wave OPO output power and pump power vs time. The total OPO output power exceeded 700 mW with a peak pump power coupled into the waveguide of 7.7 W. (b) The OPO signal and idler wavelength tuning vs pump wavelength. [after Bortz *et al.*⁹⁴]

Progress in laser diode frequency doubling in guidedwave QPM-LiTaO₃ was extended by Yamamoto *et al.*⁹⁹ who demonstrated 4.5 mW of blue light with a 13% conversion efficiency. A short time later two groups in France demonstrated a conversion efficiency of 450%/W or 1% for 2.2 mW of pump power in a 1 cm interaction length for a LiTaO₃ waveguide.¹⁰⁰ Careful control of the laser diode frequency was required for this experiment. By fabricating the waveguide in LiTaO₃ with reduced proton exchange, Suan-Yan Yi *et al.*¹⁰¹ reached a normalized efficiency of 1500%/W, which is the highest reported to date, for waveguide devices. At this efficiency 10 mW of input light was converted to 1 mW of 429 nm output in an

8 mm long interaction region. In a different material, RTA, an isomorph to KTP, Risk and Loiacono¹⁰² demonstrated 225%/Wcm² normalized doubling efficiency in a waveguide structure. 8.7 μ W of blue at 437.5 nm was generated for 21.1 mW of input. The advantage of RTA compared to KTP is that it can be electric-field poled.

The high conversion efficiency of guided-wave QPM devices allows the interaction to be engineered for other factors that may be important in device performance. For example, the narrow wavelength and temperature acceptance of the nonlinear interaction may limit practical applications of the QPM devices. Fejer *et al.*⁵⁹ suggested in their theoretical description of QPM interactions that the phase synchronism bandwidths could be artificially structured using Fourier synthesis. The phasematching acceptance bandwidth is the Fourier transformation of the nonlinear coefficient distribution or equivalently, the crystal length for a uniform nonlinear interaction length. A QPM tuning curve, up to a scale factor dependent on the dispersion, is shifted by the periodic modulation of the nonlinear coefficient and has the same bandwidth as the nonshifted structure. The approach is to artificially broaden the synchronism phasematching curve through aperiodic modification of the QPM structure.

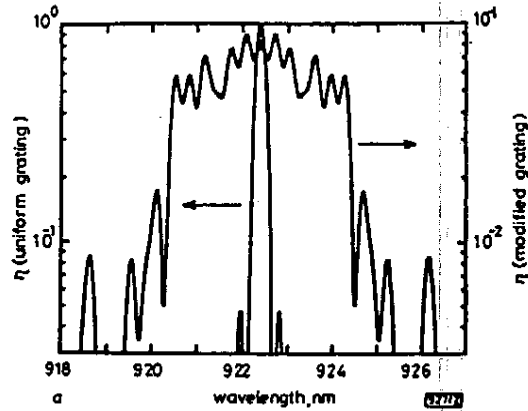
This idea was experimentally demonstrated by Bortz *et al.*¹⁰³ An analysis was presented by Fujimura *et al.*¹⁰⁴ and extended by Mizuuchi *et al.*¹⁰⁵ Details of synthesizing novel tuning curves using non-uniform QPM gratings is presented by Bortz.¹⁰³

Figure 12a shows the theoretically calculated SHG tuning curves for a uniform QPM grating and for a variably-spaced, phase-reversed QPM grating, and Fig. 12b shows the experimentally measured tuning curves from waveguides with uniform and variably-spaced phase reversed QPM gratings.

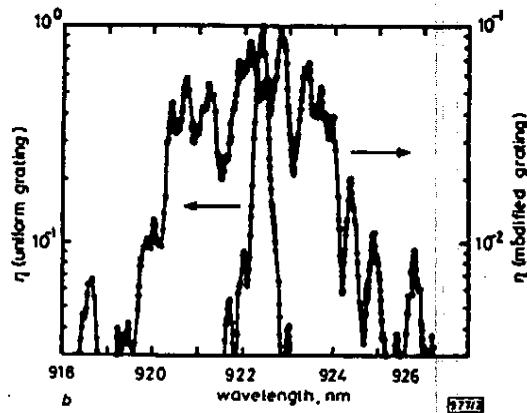
Modulation of the QPM gratings can produce sidebands and multiple phase-matching peaks in addition to the principle phasematching peak. Thus multiple output frequencies in mixers or parametric amplifiers can be generated. It is also possible, and has been demonstrated recently, that chirped QPM gratings can be used to compress frequency-chirped pulses while generating the second harmonic. This is a fundamentally different approach to pulse compression using a nonlinear interaction in a media with aperiodic QPM grating.¹⁰⁶ Control of the optical radiation also can be achieved by spatial modulation of the QPM grating to achieve modified spatial profiles of the interacting beams. G. Imeshev *et al.*¹⁰⁷ have demonstrated lateral patterning of the generated second harmonic spatial mode by using a transverse spatially-varying QPM grating to generate a flat topped gaussian beam.

5.2. Bulk Wave Quasi-Phasematched Nonlinear Devices

Nearly, simultaneously, with the demonstration of the first QPM OPO by Bortz *et al.*⁹⁴ in a waveguide, Myers *et al.*¹⁰⁸ operated the first bulk crystal QPM OPO.



(a)



(b)

Fig. 12. (a) Theoretical and (b) experimental SHG tuning curves from waveguides with uniform and variably-spaced phase reversed QPM gratings. [after Bortz Ref. 103]

The QPM OPO was pumped by a *Q*-switched Nd:YAG laser and tuned over the 1.66 to 2.95 μm spectral region. The threshold was approximately 0.1 mJ, more than one decade below the damage level of the QPM-LiNbO₃ crystal, and more than a factor of twenty below the threshold energy of a birefringently phasematched LiNbO₃ OPO.²⁷ The QPM-LiNbO₃ crystal was an electric field poled, 0.5 mm thick sample with a 31 μm period over the 5.2 mm interaction length. The low threshold of the QPM-LiNbO₃ OPO has recently allowed OPO and OPAs to be pumped by microchip lasers with threshold pump energy near 1 μJ . Zahowsky¹⁰⁹ has reported OPA operation at 1 kHz repetition rate was a 25% conversion efficiency over the tuning range from 1.4 to 4.3 μm .

The nanosecond pumped OPO was followed by a microsecond pulsed pumped QPM OPO¹¹⁰ based on a 15 mm long interaction length electric field poled LiNbO₃ crystal. This long-pulse, low-threshold, singly-resonant (SRO) QPM-LiNbO₃ OPO set the stage for a cw OPOs that were to follow.

The gain available for parametric interactions in QPM-LiNbO₃ using the d_{33} coefficient opened the possibility of low threshold operation for cw devices. The first cw QPM OPO was a laser diode pumped double resonant parametric oscillator (DRO).¹¹¹ The laser diode pumped DRO operated near degeneracy at 1.96 μm when pumped by a 977.6 nm diode laser. The measured threshold was 61 and 98 mW for 0.3 and 0.7% output couplers. The measured peak output powers were 34 mW and 64 mW for these output couplers at a pump power of 370 mW. This DRO showed the expected instabilities from cluster effect; the requirement of simultaneous resonance at the signal and idler beams.

The availability of QPM-LiNbO₃ crystal opened the possibility of difference frequency mixing for tunable infrared generation. The first mixing experiment by Goldberg *et al.*¹¹² demonstrated the advantages of QPM-LiNbO₃ of high nonlinearity, and control over the phasematching condition. Sanders *et al.*¹¹³ used two tunable diode laser sources mixed in QPM-LiNbO₃ to generation 7.1 μW of output tunable over the 3.6–4.3 μm region. The work was extended by Balakrishnan *et al.*¹¹⁴ who demonstrated 31 μW of tunable output at 4.3 μm in QPM-LiNbO₃. In this experiment, the poling period of QPM-LiNbO₃ varied from 21.0 to 22.6 μm in the transverse direction to allow the phasematching to be tuned. Petrov *et al.*¹¹⁵ used a QPM-LiNbO₃ mixer to generate tunable output in the 2160 to 2320 cm^{-1} region to detect CO, N₂O and CO₂ with a detection sensitivity of 5ppb $\text{m Hz}^{-1/2}$ in ambient air.

The extension of QPM interactions to the visible and ultraviolet require that QPM periods be reduced from 30 μm appropriate for infrared interactions to less than 6 μm required for second harmonic generation to the green or blue. One approach to shorter periods is the controlled growth of lithium niobate using yttrium doped into the melt. Using this approach the group at Nanjing University led by Duan Feng and Nai-Ben Ming made steady progress in domain control.¹¹⁶ The QPM-LiNbO₃ crystals with domain periods of less than 3 μm were grown and used in experiments for SHG to the green and blue. In one experiment a 978 nm laser diode with 500 mW of incident power was doubled to generate 1.27 mW of blue.¹¹⁷ QPM periods of 7.2 and 6.9 μm were used for third-order QPM SHG of a modelocked Ti:sapphire laser to generate 9.7 and 2.9 mW of 390 and 385 nm ultraviolet radiation for 770 mW of input power.¹¹⁸ In a recent breakthrough, W. S. Hu *et al.*¹¹⁹ showed that laser ablation growth of lithium niobate, modulated by a 70–75 V grid control voltage above the substrate, could yield controlled domain growth of LiNbO₃. This growth approach opens the possibility of preparing {001} oriented films with periodic modulations of the c -axis direction.

Electric field poling of LiNbO₃ and LiTaO₃ has been improved to the degree that 3.6 μm domain periods were demonstrated by Baron *et al.*¹²⁰ The resulting

QPM-LiTaO₃ crystal was used to generate 3 mW of blue at 2%/(Wcm) conversion for bulk interaction. Using proton exchange followed by high-voltage pulse electric field poling, Mizuuchi and Yamamoto¹²¹ demonstrated 3.3 μm periods in QPM-LiTaO₃ which allowed the generation of 340 nm light in a second order QPM interaction. LiTaO₃ is known to be transparent to 280 nm which opens the possibility of efficient generation of ultraviolet radiation to the absorption edge. Using corona discharge poling in bulk MgO:LiNbO₃, Harada and Nihei¹²² demonstrated poling of LiNbO₃ and LiTaO₃ at a 5.2 μm period. They 'frequency-doubled' a 790 mW diode laser to generate 6.7 mW of 490 nm output in a 6.5 mm long MgO:LiNbO₃ sample. Kitaoka *et al.*¹²³ used electric field poling of LiTaO₃ to form a QPM-LiTaO₃ device 6.5 mm in length to generate 10 mW of green output from an internally frequency-doubled laser-diode pumped Nd:YVO₄ laser. The sample did not suffer transverse mode distortion from photorefractive scattering. As a final example, Risk and Lau¹²⁴ used chemical patterning with electric field poling to prepare QPM-KTP samples. The waveguide device generated 0.9 mW of blue light with 91 mW of input for a normalized conversion efficiency of 24%/Wcm². This process permits in-situ monitoring of the second harmonic power during poling and the poling process is self-terminating.

The coupling of light into waveguides and the mode transformation in the nonlinear process with widely separated interacting wavelengths may have detrimental effects on the efficiency of the nonlinear process. Chou *et al.*¹²⁵ have fabricated a tapered periodic-segmented channel waveguide to ease the coupling problem and to control mode conversion for widely separated wavelengths. The segmented channel waveguide has been used to stably launch 95% of the power into the fundamental mode of a highly multimode (13 modes) guide. Further, the segmented waveguide is fabricated with two dimensional lithographic patterning followed by proton diffusion. Coupled with lithographic patterning followed by electric field poling, the segmented tapered waveguide technology brings an important capability to QPM interactions.

Photorefractive scattering is well known in oxide nonlinear materials. It was expected, and confirmed by analysis and experiments¹²⁶ that the photorefractive effects would be reduced in QPM materials. The result is that QPM-LiNbO₃ and QPM-LiTaO₃ have a much higher resistance to photorefractive damage than bulk uniformly poled crystals. Residual photorefractive scattering can be completely removed by heating the sample to approximately 100 C as verified in OPO experiments by Myers *et al.*⁵⁸

The efficiency of nonlinear frequency conversion is improved by the use of high peak powers available from mode-locked laser sources. Further, extending the wavelength range of mode locked lasers is important for many applications. In 1996, Purneri *et al.*¹²⁷ used a mode locked Nd:YLF laser to study second harmonic generation in QPM-LiNbO₃. In a cw mode locked SHG experiment 330 mW of green was generated at an average conversion efficiency of 52%. A QPM-LiNbO₃

sample of 3.2 mm length was used for 'frequency-doubling' the 2.5 psec pulses. The QPM grating with 6.35 μm period was fabricated using electric field poling with liquid electrolyte electrodes.

The picosecond pumped interaction was extended by Pruneri *et al.*¹²⁸ to a synchronously pumped OPO with pump wavelength of 523.5 nm and a tuning range from 883 to 1285 nm. The OPO generated 200 mW of average output power within a 10 μsec pulse envelope. The QPM-LiNbO₃ sample was 3.2 mm in length which was suitable for the 2 psec pump pulses. Pump depletion of 50% was observed during the 10 μsec duration of the macropulse. The synchronously pumped QPM-LiNbO₃ OPO was extended to continuous wave operation by Butterworth *et al.*¹²⁹ Here the OPO was pumped at 1.047 μm by a mode locked Nd:YLF laser. Picosecond pulses were tunable from 1.67 to 2.806 μm . The average output power level was 120 mW with a slope efficiency of 61% at 75% pump depletion when the oscillator was operated at three times threshold. The output power stability of this OPO was excellent with < 5% peak to peak variation. As noted by the authors, synchronously pumped QPM OPOs are a promising, compact and low cost source of broadly tunable radiation.

The ultrashort pulse interactions were extended by Arbore *et al.*¹³⁰ who demonstrated efficient frequency doubling of a mode locked erbium-fiber soliton laser to generate output at 777 nm with a 190 fsec pulsewidth. Arbore *et al.* showed that the characteristic interaction length for which the spectral acceptance of the SHG process is the same as the pulse bandwidth is given by

$$L_{\text{max}} = (0.44\lambda^2/\Delta\lambda)\Delta n_g^{-1} \quad (14)$$

where $\Delta\lambda$ is the full width at half maximum spectral width of the pulse and Δn_g is the group velocity mismatch between the harmonic and the fundamental waves. For transform limited pulses that are chirp free Eq. (14) reduces to the transform limited interaction length

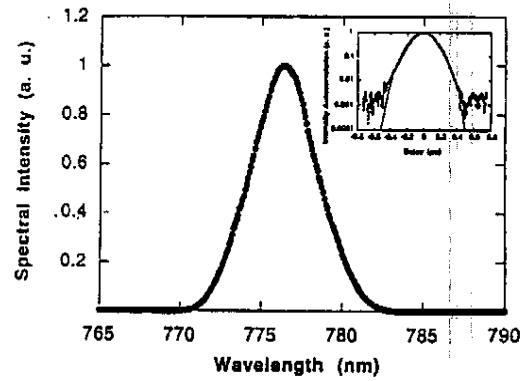
$$L_\tau = k\tau c\Delta n_g^{-1} \quad (15)$$

where τ is the pulse duration $k = 1.4$ for sech^2 pulses. Arbore *et al.*¹³⁰ define a figure of merit (FOM) for phasematched SHG of ultrashort pulses as

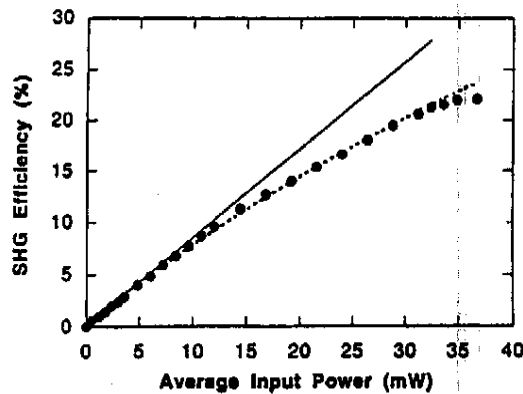
$$\text{FOM} = d_{\text{eff}}^2/(n^2\Delta n_g). \quad (16)$$

The larger nonlinear optical coefficient more than compensates for the increased group velocity dispersion of QPM-LiNbO₃. The FOM for QPM-LiNbO₃ for SHG of 1.56 μm is 710 compared to 340, 42 and 12 pm^2/V^2 for BBO, LBO and LiIO₃. For noncritically phasematched SHG interaction, the conversion efficiency is proportional to the FOM.

For confocally focussed SHG at $L = L_{\text{max}}$ the SHG efficiency is 95%/nJ compared to 6%/nJ for BBO, assuming a 100 fsec pulsewidth. The large FOM of QPM-LiNbO₃ make it the nonlinear material of choice for application to femtosecond devices such as harmonic generators, parametric generators and autocorrelators.



(a)



(b)

Fig. 13. (a) Spectral intensity of the generated 190 fsec SHG pulses at 775 nm. Inset shows the autocorrelation spectrum on a log scale. The solid curve represents the theoretical autocorrelation. (b) Internal SHG conversion efficiency vs incident $1.56 \mu\text{m}$ power. The dashed curve was obtained by averaging space and time with the input pulses, taking into account pump depletion. The solid line is 1%/mW conversion efficiency.

Figure 13a shows the spectral intensity of the generated 100 fsec SHG pulses at 775 nm. The inset shows the autocorrelation on a logarithmic scale. Figure 13b shows the internal SHG efficiency vs the internal average power at $1.56 \mu\text{m}$. The solid curve is the 1%/mW conversion efficiency for reference. The large nonlinear coefficient and the noncritical phasematching allowed by QPM-LiNbO₃ yielded a 25% conversion efficiency for SHG of 100 fsec pulses while preserving the transform limited spectral characteristics.

In an extension of the femtosecond SHG results, Galvanauskas *et al.*¹³¹ demonstrated the first femtosecond pumped QPM-LiNbO₃ parametric generator with output tunable from 1 to 3 μm when pumped by 777 nm. The OPO reached a 38% internal conversion efficiency when pumped by 220 nJ of energy. The 54 nJ

parametric generation threshold was observed and efficient operation was obtained at 200 kHz repetition rates. The output pulse length was measured by autocorrelation to be 300 fsec FWHM.

The operation of a cw singly-resonant parametric oscillator (SRO) offers many advantages in spectral control, conversion efficiency, tuning range and in stability. However, as is well known, the threshold of a SRO is approximately 200 times higher than for a DRO with the same 1% round trip losses. Thus, to reach threshold for a cw SRO requires QPM-LiNbO₃ samples that are near theoretical performance in parametric gain over a gain length of 50 mm. It is a considerable challenge to achieve uniform domain inversion with near 50% duty cycle for the required interaction lengths.

Progress in the study of electric field ferroelectric domain inversion by Miller *et al.*¹³² led him to develop a model that describes the optimized electrode pattern and applied electric field to reach self-terminated electric field poling with near 50% duty cycle. The model was first applied to producing 50 mm long QPM-LiNbO₃ samples with 30 μm periods suitable for IR OPO operation.

Myers *et al.*¹³³ demonstrated cw SRO operation with a 3W threshold power for a 1.064 μm Nd:YAG pump. The cw SRO used a 50 mm long QPM-LiNbO₃ gain element. The output power levels generated were greater than 2.5 W at 3.3 μm . The device was tunable over the 1.4–1.6 and 3.1–4.0 μm range. The SRO spectral characteristics were studied by Bosenberg *et al.*¹³⁴ As predicted by Harris³ twenty-five years earlier, the SRO operated in a single axial mode on the resonated signal wave even when the pump was multi-axial mode. The cw SRO operated with less than 1% amplitude fluctuation when the signal wave was of single axial mode. The maximum output power was 1.25 W at 3.25 μm and 0.36 W at 1.57 μm for 13 W of pump power.

Bosenberg *et al.*¹³⁵ extended the cw SRO performance to achieve a remarkable 93% pump depletion for the Nd:YAG pumped QPM-LiNbO₃ singly-resonant OPO. The SRO operated with 86% of the converted pump photons as useful idler photons at 3.25 μm . This SRO was operated in both a standing wave and in a ring cavity. The performance of the SRO was improved with the ring cavity configuration reaching 93% pump depletion at 2.4 times threshold. The idler output power reached 3.7 W for an input pump power of 14 W. An internal etalon within the SRO resonator allowed tuning over a 5 cm^{-1} range with discrete mode hops at each axial mode. A multiple grating QPM-LiNbO₃ element with grating periods stepped in quarter micron increments from 28.0 to 29.75 μm was also tested in the cw SRO. Tuning was achieved over a range from 1.45–1.60 and 3.95–3.25 μm by translating the QPM crystal transverse to the SRO resonator axis.

The power of lithographic patterning of QPM-LiNbO₃ gain elements is illustrated by the multigrating QPM OPO demonstrated by Myers *et al.*¹³⁶ Beginning with a 0.5 mm thick wafer of LiNbO₃, Myers designed and then prepared an electric-field poled 27 mm long interaction length QPM-LiNbO₃ chip with 25 OPO gratings, each 500 μm wide. The grating periods ranged from 26 to 32 μm thus allowing

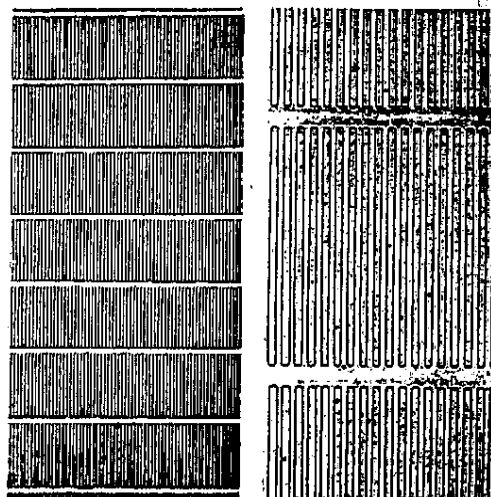
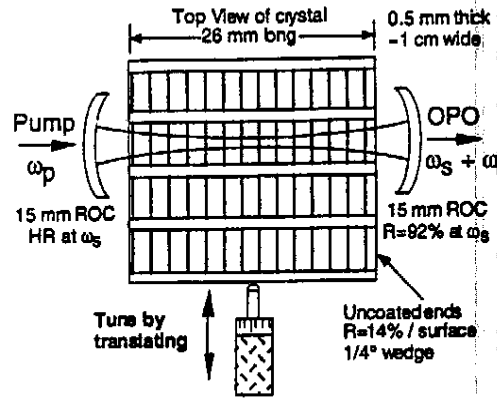


Fig. 14. A photograph of the $+z$ surface of a 0.5 mm thick QPM-LiNbO₃ multiple grating chip etched in HF acid to reveal the domain structure. The lithographic mask consisted of 25 gratings with periods from 26–32 μm steps. On the right is an enlarged section of the 29 μm grating. The length of the finished gratings was 26 mm.

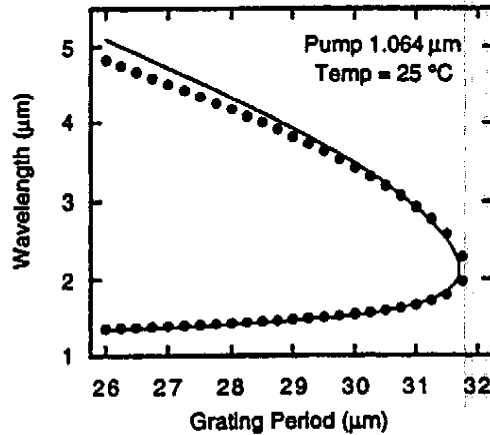
tuning across the 1.4 to 4.8 μm spectral range when pumped by an acousto-optic Q -switched Nd:YAG laser source.

Figure 14 shows a photograph of a section of the QPM-LiNbO₃ multigrating domain array. On the left are seven gratings of 500 μm width separated by 50 μm . On the right is an enlargement of the 29 μm period grating, showing in detail the exquisite uniformity of the electric field poling process. Figure 15a shows a schematic of the experimental setup for the multigrating QPM OPO. The OPO was tuned by translating the crystal perpendicular to the OPO resonator optical axis. No realignment was needed and all grating sections oscillated with good efficiency. Figure 15b shows the OPO tuning range vs the grating period. The tuning gaps can be covered by a small shift in the crystal temperature. In the future the gratings can be fabricated with closer pitch spacing or with a wedged pitch for continuous tuning. This multigrating OPO had a threshold of 6 μJ for the 26 mm interaction length. The OPO reached 70% pump depletion at 8 times threshold and operated well below the damage level of the QPM-LiNbO₃ crystal.

Continued progress in electric field poling by Miller *et al.*¹³² led to the preparation of a 5.3 cm long, 5.6 μm domain-period first order QPM-LiNbO₃ sample for bulk cw SHG of a Nd:YAG laser. Miller *et al.*¹³⁷ reported single pass cw SHG experiment generated 2.7 W of 532 nm output for 6.5 W of 1064 nm input. This 42% single pass conversion efficiency is the highest reported to date and represents a significant breakthrough in nonlinear optical frequency conversion. Figure 16a shows the temperature phase matching curve. The dots are data points and the solid line is theory. The measurement showed that the QPM-LiNbO₃ sample phase-



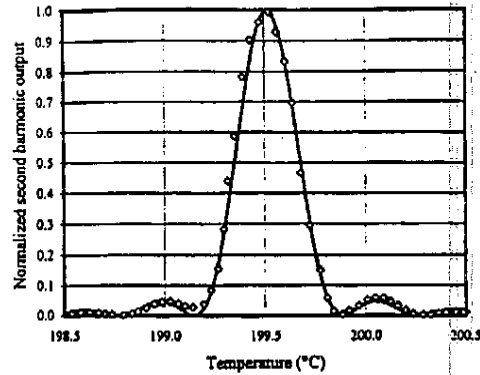
(a)



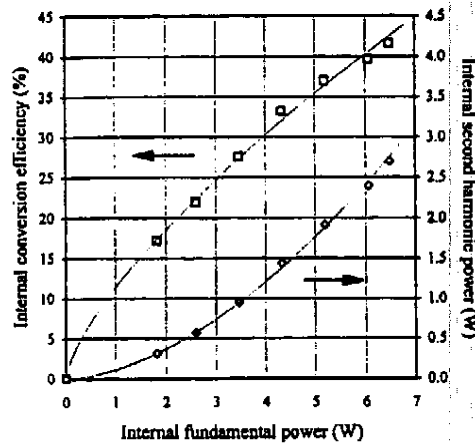
(b)

Fig. 15. (a) Schematic of the multigrating OPO experiment showing 26 mm long multigrating gain regions within the OPO resonator. Tuning was accomplished by translating the gratings through the pump beam. No realignment was necessary. (b) The multigrating OPO tuning curve through 24 grating sections that were phasematched. The tuning ranged from 1.36 to 4.83 μm . The OPO threshold was 6 μJ for the 7 nsec long Nd:YAG pump pulses.

matched over its entire 5.3 cm length and that the duty factor was near 50% since the effective nonlinear coefficient was 14 pm/V which is 80% of the ideal value. Figure 16b shows the SHG internal conversion efficiency and the generated SHG power vs the internal fundamental power. The generated power reached 2.7 W at a conversion efficiency of 42% for single pass cw second harmonic generation. This result led to the possibility of directly 'frequency-doubling' laser diodes for the generation of red, green and blue output for display applications.



(a)



(b)

Fig. 16. (a) Quasi-phasematching temperature tuning curve for a 5.3 cm long $6.5 \mu\text{m}$ domain-period first order SHG experiment. The dots are experimental data and the solid line is theory showing that the crystal phasematched over the entire interaction length with an effective nonlinear coefficient of 14 pm/V which is 80% of the ideal value. (b) Internal second harmonic generation efficiency and output power vs incident internal fundamental power. 2.7 W of 532 nm was generated for 6.5 W of incident power for a 42% conversion efficiency. This is the highest single pass conversion efficiency for cw SHG reported to date.

In a related experiment, Batchko *et al.*¹³⁸ demonstrated a 532 nm cw-pumped single-resonant OPO based on the same 5.2 cm long first order QPM-LiNbO₃ samples. The cw SRO had a threshold of less than 1 W and operated with a 64% quantum efficiency. At three time threshold the pump depletion reach 60% and the idler output power was 0.9 W. Work is continuing on this OPO with the goal of intracavity frequency doubling the signal wave to generate blue and the idler wave to generate red for possible application to RGB displays.¹³⁹

6. Future Directions

Progress in QPM nonlinear materials and fabrication capability has led to the exploration of other nonlinear interactions and applications. For example, the generation of squeezed light was demonstrated by Anderson *et al.*¹⁴⁰ and by Serkland *et al.*¹⁴¹ in 1995. Serkland *et al.* used a QPM-LiNbO₃ guided wave parametric amplifier pumped by 0.5 W of peak power at 532 nm. The experiment demonstrated 14% squeezing which correlated well to the measured phase sensitive amplification and 40% detector efficiency. In a recent experiment, Lovering *et al.*¹⁴² demonstrated noiseless optical amplification in a QPM-LiNbO₃ phase-sensitive optical parametric amplifier. Work is now in progress on improved squeezing using the recently prepared electric field poled QPM-LiNbO₃ gain elements.

The large nonlinearity of the QPM interaction allows the possibility to revisit the idea of applying cascaded second order nonlinearity to demonstrate phase shift and optical switching as first proposed by Stegemann in 1988.¹⁴³ Asobe *et al.*¹⁴⁴ used sum and difference frequency interactions in a QPM-LiNbO₃ crystal 10 mm in length. Optical switching was observed for gate power levels of 2 kW. Vidakovic *et al.*¹⁴⁵ measured values for $n_n^{cascade}$ of 2.39×10^{-13} and -2.37×10^{-13} in the cascaded $\chi^{(2)}$ interaction in QPM-LiNbO₃. These values are one order of magnitude larger than for KTP and three orders of magnitude larger than for silica fibers.

The QPM interaction can also be applied to beam control, beam focusing and to beam steering. The ability to lithographically pattern the QPM structure allows the consideration of prism and lens arrays for these applications. Chiu *et al.*¹⁴⁶ demonstrated beam deflection in QPM-KTP with prisma arrays. Yamada *et al.*¹⁴⁷ have demonstrated lenslet arrays for focal length control, optical switching, and beam deflection. These early results show that the possibilities for extending the use of QPM interactions to control optical beams is open for further exploration and development.

The inversion of ferroelectric domains to periodically invert the sign of the nonlinear coefficient is one example of modulating a material to achieve an enhanced nonlinear optical interaction. Materials can be tailored at various scales ranging from the atomic to the microscopic and by various means including modulated growth, modulated structure, and patterned growth. For example, significant progress has been made in the growth of quantum well structures for enhanced nonlinear coefficients in the infrared since the first quantum well nonlinear response was measured by Fejer *et al.* in 1989.¹⁴⁸ In recent work, H. C. Chui *et al.*¹⁴⁹ have demonstrated tunable mid-infrared generation by difference frequency mixing of diode laser wavelengths in InGaAs/AlAs quantum wells. The nonlinearity of the quantum wells was measured to be 12 nm/V or more than 65 times the bulk nonlinear response of GaAs for the near infrared mixing process. A CO₂ laser was frequency doubled in the intersubband quantum wells with an effective nonlinearity of 52 nm/V. These results indicate the possibility of QPM device interactions in the mid-infrared using the large nonlinear response of the quantum well structures.

At a large scale, patterned growth of periodically inverted GaAs has been proposed by Angell *et al.*¹⁵⁰ Laterally patterning the $\langle 111 \rangle$ and $\langle 100 \rangle$ oriented regions of CdTe on GaAs provide a means of achieving quasi-phases matching in these semiconductor materials. The patterned CdTe layer is shown to be a suitable template for the growth of wide gap ZnSe and ZnTe. In a similar vein, Yoo *et al.*¹⁵¹ used wafer bonding to create an alternate template substrate for the growth of a periodic crystal inversion to achieve quasi-phases matching in AlGaAs. The results are potentially applicable to wavelength division multiplexing networks.

Finally, at the macroscale, Gordon *et al.*¹⁵² proposed to wafer bond alternately inverted GaAs plates for quasi-phases matched interactions in the mid-infrared. Early results showed the QPM interaction would remain in phases matched for nine layers. Recent results have led to wafer bonding losses being reduced to less than 0.1% per layer and to a stack of wafer bonded material with 30 to 50 layers being prepared. Wafer bonded QPM GaAs offers the possibility of high average power nonlinear frequency conversion. Further, wafer bonded GaAs is an optically isotropic medium with a very wide angular and temperature acceptance range which may prove to be useful for infrared generation and infrared up-conversion applications.

These examples of alternate materials systems for quasi-phases matching show that there remain opportunities for further progress. The ability to engineer the nonlinear material to meet the application and to optimize the nonlinear interaction has led to rapid progress in both materials and devices. However, the leverage of mass production made possible by lithographic patterning with subsequent domain inversion has led to a rapid transition from nonlinear crystals that cost thousands of dollars to nonlinear chips that cost less than one dollar each. For the first time, more than thirty years after the first suggestion of quasi-phases matching by Bloembergen,⁶ nonlinear chips can be engineered and mass produced at a cost that is acceptable for widespread consumer applications. It is too early to tell what devices will meet future needs, but it is evident that the powerful tools developed for processing silicon integrated circuits will have a lasting effect on nonlinear optics.

Acknowledgements

This paper summarizes a seminar presented at the Rem V. Khokhlov 70th Jubilee, October 14-19, 1996, Moscow, Russia. The paper is dedicated to Rem V. Khokhlov, Sergie Akhmanov, and Sasha Kovrigin and to the early pioneers of nonlinear optics. My thanks to M. M. Fejer for help with the preparation of the manuscript. The work is supported by the Advanced Research Projects Agency through the Center for Nonlinear Optical Materials at Stanford University.

References

1. N. Bloembergen, *Nonlinear Optics*, Benjamin, New York (1965).
2. S. A. Akhmanov and R. V. Khokhlov, *Problems in Nonlinear Optics*, Akad. Nauk. USSR, Moscow (1964) English edition 1973, Gordon and Breach, New York (1973).
3. S. E. Harris, *Tunable Optical Parametric Oscillators Proc. IEEE* **57**, 2096 (1969).

4. P. A. Franken, A. E. Hill, C. W. Peters and G. Weinrich, *Phys. Rev. Lett.* **7**, 118 (1961).
5. D. A. Kleinman, *Phys. Rev.* **126**, 1977 (1962); J. A. Giordmaine, *Phys. Rev. Lett.* **8**, 19 (1962); P. D. Miller, R. W. Terhune, N. Nisenhoff and C. M. Savage, *Phys. Rev. Lett.* **8**, 21 (1962); S. A. Akhmanov, A. I. Kovrigin, R. V. Khokhlov and O. N. Chunaev, *Zh. Eksp. Theor. Fiz.* **45**, 1336 (1963), Transl. *Sov. Phys. JETP* **18**, 919 (1966).
6. J. A. Armstrong, N. Bloembergen, J. Ducuing and P. S. Pershan, *Phys. Rev.* **127**, 1918 (1962).
7. R. H. Kingston, *Proc. IRE* **50**, 472 (1962).
8. N. M. Kroll, *Phys. Rev.* **127**, 1207 (1962).
9. S. A. Akhmanov and R. V. Khokhlov, *Zh. Eksp. Theor. Fiz.* **43**, 351 (1962); Transl. *Sov. Phys. JETP* **16**, 252 (1963).
10. J. A. Giordmaine and R. C. Miller, *Tunable Coherent Parametric Oscillation in LiNbO₃ at Optical Frequencies*, *Phys. Rev. Letts.* **14**, 973 (1965).
11. S. A. Akhmanov, A. I. Kovrigin, V. A. Kosolov, A. S. Piskarskas, V. V. Fadeev and R. V. Khokhlov, *Tunable Parametric Oscillator Based on KDP Crystal*, *JETP Letts.* **3**, 372 (1966).
12. A. G. Akhmanov, S. A. Akhmanov, R. V. Khokhlov, A. I. Kovrigin, A. S. Piskarskas and A. P. Sukhorukov, *Parametric Interactions in Optics and Tunable Light Oscillators*, *IEEE Journ Quant. Electr.* **QE-4**, 828 (1968).
13. G. D. Boyd and A. Ashkin, *Phys. Rev.* **146**, 187 (1966).
14. R. L. Byer, M. K. Oshman, J. F. Young and S. E. Harris, *Visible cw Parametric Oscillator*, *Appl. Phys. Letts.* **13**, 110 (1968).
15. R. L. Byer, A. Kovrigin and J. F. Young, *A cw ring-cavity parametric oscillator*, *App. Phys. Letts.* **15**, 136 (1969).
16. W. H. Louisell, A. Yariv and A. E. Siegman, *Quantum Fluctuations and Noise in Parametric Processes I*, *Phys. Rev.* **124**, 1646 (1961).
17. S. E. Harris, M. K. Oshman and R. L. Byer, *Phys. Rev. Letts.* **18**, 732 (1967).
18. T. G. Giallorenzi and C. L. Tang, *Phys. Rev.* **166**, 225 (1968).
19. D. A. Kleinman, *Phys. Rev.* **174**, 1027 (1968).
20. D. N. Klyshko, *JETP Letts.* (1967).
21. J. A. Giordmaine, *Physics Today* **22**, 38 (1969).
22. R. L. Byer, *Nonlinear Optical Phenomena and Materials*, in *Annual Review of Materials Science*, Vol. 4 (Annual Reviews, Inc. Palo Alto, CA, 1974) p. 147.
23. N. Bloembergen, *Apparatus for Converting Light Energy from One Frequency to Another*, U.S. Patent 3,384,433 filed July 9, 1962 and issued May 21, 1968.
24. H. Kildal and R. L. Byer, *Comparison of Laser Methods for the Remote Detection of Atmospheric Pollutants*, invited paper, *Proc. IEEE* **59**, 1644 (1971).
25. R. L. Byer, *Parametric Oscillators and Nonlinear Materials*, in *Treatise in Quantum Electronics*, Vol. I, H. Rabin and C. L. Tang, eds., Academic Press, New York (1973).
26. R. L. Herbst, H. Komine and R. L. Byer, *A 200 mJ Unstable Resonator Nd:YAG Oscillator*: *Opt. Commun.* **21**, 5 (1977).
27. S. J. Brosnan and R. L. Byer, *Optical Parametric Oscillator Threshold and Linewidth Studies*, *IEEE J. Quantum Electron.* **QE-15**, 415 (1979).
28. R. A. Baumgartner and R. L. Byer, *Optical Parametric Amplification*, *IEEE J. Quantum Electron.* **QE-15**, 432 (1979).
29. R. L. Byer, R. L. Herbst, R. S. Feigelson and W. L. Kway, *Growth and Applications of [01.4] LiNbO₃*, *Opt. Commun.* **12**, (1974); see also R. L. Byer and R. L. Herbst, *Tunable Electromagnetic Oscillator Using [01.4] Grown LiNbO₃ and Method*, U.S. Patent 3,922,561 issued Nov 25, 1975.

30. R. A. Baumgartner and R. L. Byer, *Remote SO₂ Measurements at 4 μm with a Continuously Tunable Source*, *Opt. Lett.* **2**, 163 (1978).
31. R. A. Baumgartner and R. L. Byer, *Continuously Tunable IR LIDAR with Applications to Remote Measurements of SO₂ and CH₄*, *Appl. Opt.* **17**, 3555 (1978).
32. M. Endemann and R. L. Byer, *Remote single-ended measurements of atmospheric temperature and humidity at 1.77 μm using a continuously tunable source*, *Opt. Lett.* **5**, 452 (1980); M. Endemann and R. L. Byer, *Simultaneous Remote Measurements of Atmospheric Temperature and Humidity using a Continuously Tunable IR LIDAR*, *Appl. Opt.* **20**, 3211 (1981).
33. R. L. Byer, *Parametric Oscillators and Nonlinear Materials*, in *Nonlinear Optics*, P. G. Harper and B. S. Wherett, eds. (Academic Press, London, 1977) p. 47.
34. R. F. Begley, A. B. Harvey and R. L. Byer, *Coherent Anti-Stokes Raman Spectroscopy*, *Appl. Phys. Lett.* **235**, 387 (1974).
35. M. A. Henesian, R. L. Byer and L. Kulevskii, *Collisionally Narrowed Lineshape of Raman Q-Branch Lines of H₂ and D₂*, *Bull. Am. Phys. Soc.* **21**, No. 11, Abs BC1, p. 1287 (1976).
36. M. D. Duncan, P. Osterlin and R. L. Byer, *Pulsed supersonic Molecular Beam Coherent Anti Stokes Raman Spectroscopy of C₂H₂*, *Opt. Lett.* **6**, 90 (1981).
37. M. A. Henesian, L. A. Kulevskii and R. L. Byer, *CW High Resolution CAR Spectroscopy of H₂, D₂ and CH₄*, *Opt. Commun.* **18**, 225 (1976).
38. N. I. Koroteev, M. Endemann and R. L. Byer, *Resolved Structure within the Broad Band Vibrational Raman Line of Liquid H₂O from Polarization Coherent Anti-Stokes Raman Spectroscopy*, *Phys. Rev. Lett.* **43**, 398 (1979).
39. C. Chen, B. Wu, A. Jiang and G. You, *A new type ultraviolet SHG crystal B-BaB₂O₄*, *Sci. Sin. Ser. B28*, 235 (1985); C. T. Chen, R. C. Eckardt, Y. X. Fan and R. L. Byer, *Recent Developments in Beta Barium Borate*, *Proc. SPIE 681, Laser and Nonlinear Optical Materials*, 12 (1986).
40. Y. X. Fan, R. C. Eckardt, R. L. Byer, C. Chen and A. Jiang, *Beta phase barium borate optical parametric oscillator*, presented at *CLEO 86*, post deadline paper ThT4: Y. X. Fan, R. C. Eckardt, R. L. Byer, J. Nolting and R. Wallenstein, *Visible BBO optical parametric oscillator pumped by 355 nm by a single-axial-mode pulsed source*, *Appl. Phys. Lett.* **53**, 2014 (1988).
41. C. L. Tang, W. R. Bosenberg, T. Ukachi, R. J. Lane and L. K. Cheng, *Optical Parametric Oscillators*, Invited paper, *Proceedings of the IEEE*, **80**, 365 (1992).
42. J. G. Haub, M. J. Johnson and B. J. Orr, *Continuously tunable injection-seeded beta Barium borate optical parametric oscillator: spectroscopic applications*, *Appl. Phys. Lett.* **58**, 1718 (1991); see also M. J. Johnson, J. G. Haub and B. J. Orr, *Opt. Lett.* **20**, 1277 (1995); J. G. Haub, M. J. Johnson, A. J. Powell and B. J. Orr, *Opt. Lett.* **20**, 1637 (1995); J. G. Haub, R. M. Hentschel, M. J. Johnson and B. J. Orr, *J. Opt. Soc. Am.* **B12**, 2128 (1995).
43. B. K. Zhou, T. Kane, G. Dixon and R. L. Byer, *Efficient, Frequency Stable Laser Diode Pumped Nd:YAG Lasers*, *Opt. Lett.* **10**, 62 (1985); R. L. Byer, *Diode-Laser Pumped Solid-State Lasers*, *Science* **239**, 742 (1987).
44. T. Kane and R. L. Byer, *Monolithic Unidirectional, Single Mode Nd:YAG Ring Laser*, *Opt. Lett.* **10**, 65 (1985); A. C. Nilsson, E. K. Gustafson and R. L. Byer, *Eigenpolarization Theory of Monolithic Nonplanar Ring Oscillators*, *IEEE J. Quant. Electr.* **25**, 767 (1989).
45. T. Y. Fan, G. Dixon and R. L. Byer, *Efficient GaAlAs Diode-Laser-Pumped Operation of Nd:YLF at 1.047 with Intracavity Doubling to 523.6 nm*, *Opt. Lett.* **11**, 204 (1986).

46. W. J. Kozlovsky, C. D. Nabors and R. L. Byer, *Efficient Second Harmonic Generation of a Diode-Laser-Pumped cw Nd:YAG Laser Using Monolithic MgO:LiNbO₃ External Resonant Cavities*, *IEEE J. Quant. Electron.* **24**, 913 (1988).
47. W. J. Kozlovsky, C. D. Nabors, R. C. Eckardt and R. L. Byer, *Monolithic MgO:LiNbO₃ doubly resonant optical parametric oscillator pumped by a frequency doubled diode laser pumped Nd:YAG laser*, *Opt. Lett.* **14**, 66 (1989); C. D. Nabors, R. C. Eckardt, W. J. Kozlovsky and R. L. Byer, *Efficient, single-axial-mode operation of a monolithic MgO:LiNbO₃ optical parametric oscillator*, *Opt. Lett.* **14**, 1134 (1989).
48. C. D. Nabors, S. T. Yang, T. Day and R. L. Byer, *Coherence properties of a doubly-resonant monolithic optical parametric oscillator*, *J. of Opt. Soc. Am.* **B7**, 815 (1990).
49. R. C. Eckardt, C. D. Nabors, W. J. Kozlovsky and R. L. Byer, *Optical parametric oscillator frequency tuning and control*, *J. Opt. Soc. Am.* **B8**, 646 (1991).
50. R. C. Eckardt, H. Masuda, Y. X. Fan and R. L. Byer, *Absolute and relative nonlinear optical coefficients of KDP, KD*P, BaB₂O₄, LIO₃, MgO:LiNbO₃, and KTP measured by phasematched second-harmonic generation*, *IEEE J. Quant. Electr.* **26**, 922 (1990).
51. S. Schiller and R. L. Byer, *Quadruply resonant optical parametric oscillation in a monolithic total-internal-reflection resonator*, *J. Opt. Soc. Am.* **B10**, 1696 (1993).
52. D. K. Serkland, R. C. Eckardt and R. L. Byer, *Continuous wave total-internal-reflection optical parametric oscillator pumped at 1064 nm*, *Opt. Lett.* **19**, 1046 (1994).
53. A. Nilsson, *Eigenpolarization Theory and Experimental Linewidth Study of Monolithic Nonplanar Ring Oscillators*, PhD Thesis, Stanford University 1989.
54. C. D. Nabors, A. D. Farinas, T. Day, E. K. Gustafson and R. L. Byer, *Injection Locking of a 13 W cw Nd:YAG ring laser*, *Opt. Lett.* **14**, 1189 (1989).
55. S. T. Yang, R. C. Eckardt and R. L. Byer, *1.9 W cw ring-cavity KTP singly resonant optical parametric oscillator*, *Opt. Lett.* **19**, 475 (1994); S. T. Yang, R. C. Eckardt and R. L. Byer, *Power and Spectral Characteristics of Continuous-Wave Parametric Oscillators: the Doubly to Singly Transition*, *J. Opt. Soc. Am.* **B10**, 1684 (1993).
56. R. L. Byer and A. Piskarskas, feature editors, *Optical Parametric Oscillation and Amplification*, *J. Opt. Soc.* **B10**, 1655 (1993).
57. W. R. Bosenberg, R. C. Eckardt, feature editors, *Optical Parametric Devices*, *J. Opt. Soc. Am.* **B12**, 2084 (1995).
58. L. E. Myers, R. C. Eckardt, M. M. Fejer, R. L. Byer, W. R. Bosenberg and J. W. Pierce, *Quasi-phasematched optical parametric oscillators in bulk periodically poled LiNbO₃*, *J. Opt. Soc. Am.* **12**, 2102 (1995).
59. M. M. Fejer, G. A. Magel, D. H. Jundt and R. L. Byer, *Quasi-Phasematched Second Harmonic Generation: Tuning and Tolerances*, *IEEE J. Quant. Electr.* **28**, 2631 (1992).
60. R. L. Byer, *Quasi-Phasematched Nonlinear Materials and Applications to Devices*, in *Nonlinear Optics*, Vol. 7, p. 235 (1994) Gordon and Breach Science Publications.
61. D. Feng, N. B. Meng, J. F. Hong, Y. S. Yang, Z. Z. Yang and Y. N. Wang, *Appl. Phys. Lett.* **37**, 607 (1980).
62. A. Feisst and P. Koidl, *Appl. Phys. Lett.* **47**, 1125 (1985).
63. A. L. Aleksandrovskii, I. I. Naumova and V. V. Tarasenko, International Symposium on Domain Structure of Ferroelectrics and related materials (ISFD - 2) 7-10 July 1992.
64. M. M. Fejer, *Single Crystal fibers: growth dynamics and nonlinear optical interactions*, PhD thesis Stanford University 1976; M. M. Fejer, J. L. Nightengale, G. A. Magel and R. L. Byer, *Rev. Sci. Instrum.* **55**, 1791 (1984).

65. Y. S. Luh, R. S. Feigelson, M. M. Fejer and R. L. Byer, *J. Crystal Growth* **78**, 135 (1986); Y. S. Luh, M. M. Fejer, R. L. Byer and R. S. Feigelson, *J. Crystal Growth* **85**, 264 (1987).
66. G. A. Magel, M. M. Fejer and R. L. Byer, *Appl. Phys. Lett.* **56**, 108 (1990); G. A. Magel, *Optical Second Harmonic Generation in Lithium Niobate Fibers*, PhD thesis, Stanford University 1990.
67. D. H. Jundt, G. A. Magel, M. M. Fejer and R. L. Byer, *Appl. Phys. Lett.* **59**, 2657 (1991); D. H. Jundt, *Lithium Niobate: single crystal fiber growth and quasi-phasesmatching*, PhD thesis Stanford University 1991 (available as Ginzton Lab report #4855).
68. S. Miyazawa, *J. Appl. Phys.* **50**, 4599 (1979).
69. K. Nakamura, H. Ando and H. Shimizu, *Proc. 1986 Ultrasonics Symposium*, pp. 719–722.
70. E. J. Lim, M. M. Fejer and R. L. Byer, *Electron. Lett.* **25**, 174 (1989); E. J. Lim, M. M. Fejer, R. L. Byer and W. J. Kozlovsky, *Electron. Lett.* **25**, 731 (1989).
71. J. Webjorn, F. Laurell and G. Arvidsson, *IEEE Photonics Tech. Lett.* **1**, 316 (1989).
72. J. D. Bierlein, D. B. Laubacher, J. B. Brown and C. J. van der Poel, *Appl. Phys. Lett.* **56**, 1725 (1990).
73. C. J. van der Poel, J. D. Bierlein and J. B. Brown, *Appl. Phys. Lett.* **57**, 2074 (1990).
74. E. J. Lim, S. Matsumoto and M. M. Fejer, *Noncritical phase matching for guided-wave frequency conversion*, *Appl. Phys. Lett.* **57**, 2294 (1990).
75. M. M. Fejer, *Nonlinear Frequency Conversion in Periodically-Poled Ferroelectric Waveguides*, in *Guided Wave Nonlinear Optics*, ed. by D. B. Ostrowsky and R. Reinisch, Kluwer Academic Publishers, The Netherlands (1992) pp. 133–145.
76. Martin M. Fejer, *Nonlinear Optical Frequency Conversion*, *Physics Today* (May 1994) p. 25.
77. L. L. Pendergrass, *J. Appl. Phys.* **62**, 231 (1987).
78. P. W. Haycock and P. D. Townsend, *Appl. Phys. Lett.* **48**, 698 (1986).
79. H. Ito, C. Takyu and H. Inaba, *Electron. Lett.* **27**, 1211 (1991); H. Ito, in *Nonlinear Optics*, ed. by S. Miyata, Elsevier Science Publishers, 1992, pp. 495–500; H. Ito, *Periodic domain reversal structures written by electron irradiation and their quasi-phasesmatching*, in *Review of Laser Engineering* **20**, 236 (1992).
80. M. Yamada, N. Nada and K. Watanabe, *Fabrication of periodically reversed domain structure for second harmonic generation in LiNbO₃ by applying voltage*, paper TuC2 Integrated Photonics Research Topical Meeting, New Orleans, Louisiana, April 13–16, 1992; M. Yamada, N. Nada, M. Saitoh and K. Watanabe, *Appl. Phys. Lett.* **62**, 435 (1993).
81. I. Camlibel, *J. Appl. Phys.* **40**, 1691 (1969).
82. N. F. Evlanova, PhD Thesis, Moscow University (1978).
83. A. M. Prokhorov and Yu S. Kuz'minov, *Physics and Chemistry of Crystalline Lithium Niobate*, Adam Hilger, New York (1990).
84. L. E. Myers, G. D. Miller, M. L. Bortz, R. C. Eckardt, M. M. Fejer and R. L. Byer, *Quasi-phasesmatched 1.064 μm pumped optical parametric oscillator in bulk periodically poled LiNbO₃*, paper PD8, *IEEE Conference on Nonlinear Optics: Materials, Fundamentals, and Applications*, Waikoloa, Hawaii, July 25–29, (1994).
85. J. Webjorn et al., *Quasi-phasesmatched blue light generation in bulk lithium niobate, electrically poled via periodic liquid electrodes*, *Electronics Letters* **30**, 894 (1994).
86. W. K. Burns et al., *Second Harmonic generation in field poled quasi-phasesmatched, bulk LiNbO₃*, *IEEE Photonics Technology Lett.* **6**, 252 (1994).

87. L. E. Myers, *Quasi-Phasematched Optical Parametric Oscillators in Bulk Periodically Poled Lithium Niobate*, PhD Dissertation, Department of Electrical Engineering, Stanford University, Stanford, CA 1995 (available as Ginzton Laboratory report No. 5396) (1995).
88. L. E. Myers, *Increasing the aperture of electric-field periodically poled LiNbO₃*, *CLEO 96*, Anaheim, CA 9, 339 (1996).
89. K. Yamamoto and K. Mizuuchi, *IEEE Photon Technol. Lett.* 4, 435 (1992).
90. M. G. Roelofs, F. Laurell and J. D. Bierlein, in *Compact Blue-Green Lasers*, Technical Digest (Optical Society of America, Washington DC, 1992), p. 127.
91. M. L. Bortz and M. M. Fejer, *Opt. Lett.* 17, 704 (1992).
92. E. J. Lim, S. Matsumoto and M. M. Fejer, *Appl. Phys. Lett.* 57, 2294 (1990).
93. M. L. Bortz, S. J. Field, M. M. Fejer, D. W. Nam, R. G. Waarts and D. F. Welch, *Noncritical Quasi-phasematched Second Harmonic Generation in an Annealed Proton-Exchanged LiNbO₃ Waveguide*, *IEEE Trans. on Quantum Electr.* 30, 2953 (1994).
94. M. L. Bortz, M. A. Arbore and M. M. Fejer, *Quasi-phasematched optical parametric amplification and oscillations in periodically poled LiNbO₃ waveguides*, *Opt. Lett.* 20, 49 (1995).
95. M. A. Arbore and M. M. Fejer, *Singly resonant optical parametric oscillation in periodically poled lithium niobate waveguides*, *Opt. Lett.* 22, 151 (1997).
96. K. Mizuuchi and K. Yamamoto, *Opt. Review* 1, 100 (1994).
97. K. Yamamoto, K. Mizuuchi, H. Hara, Y. Kitaoka and M. Kato, *Optical Review* 1, 88 (1994).
98. J. Feng et al., *Harmonic generation in an optical Fibonacci superlattice*, *Phys. Rev.* B41, 5578 (1990); Y. Y. Zhu et al., *Second-harmonic generation in a Fibonacci optical superlattice and the dispersive effect of the refractive index*, *Phys. Rev.* B42, 3676 (1990).
99. K. Yamamoto, K. Mizuuchi, Y. Kitaoka and M. Kato, *Highly efficient quasi-phasematched second-harmonic generation by frequency doubling of a high-frequency superimposed laser diode*, *Opt. Lett.* 20, 273 (1995).
100. A. Azouz, N. Steimakh, J.-M. Lourtioz, D. Delacourt, D. Papillon and J. Lehoux, *High second-harmonic conversion efficiency of quasi-phasematched LiTaO₃ waveguides pumped by single-mode pulsed AlGaAs laser diodes*, *Appl. Phys. Lett.* 67, 2263 (1995).
101. Sang-Yun Yi, Sang-Yung Shin, Yong-Sung Jin and Yung-Sung Son, *Second-harmonic generation in a LiTaO₃ waveguide domain-inverted by proton exchange and masked heat treatment*, *Appl. Phys. Lett.* 68, 2493 (1996).
102. W. P. Risk and G. M. Loiacono, *Periodic poling and waveguiding frequency doubling in RbTiOAsO₄*, *Appl. Phys. Lett.* 69, 311 (1996).
103. M. L. Bortz, M. Fujimura and M. M. Fejer, *Increased acceptance bandwidth for quasi-phasematched second-harmonic generation in LiNbO₃ waveguides*, *Electr. Lett.* 30, 34 (1994); M. L. Bortz, *Quasi-Phasematched Optical Frequency Conversion in Lithium Niobate Waveguides*, PhD Dissertation, submitted to the Department of Applied Physics, Stanford University, Stanford, CA 94305 (available as Ginzton Laboratory report No. 5259) (1994).
104. M. Fujimura, T. Suhara, H. Nishihara, M. L. Bortz and M. M. Fejer, *Tuning Bandwidth Enhancement in Waveguide Optical Second-Harmonic Generation Device Using Phase-Reversed Quasi-Phasematching Grating*, *Elec. and Commun. in Japan*, part 2, 78, 20 (1995).
105. K. Mizuuchi, K. Yamamoto, M. Kato and H. Sato, *Broadening of the Phasematching Bandwidth in Quasi-Phasematched Second-Harmonic Generation*, *IEEE J. Quant. Electr.* 30, 1596 (1995).

106. M. A. Arbore, O. Marco and M. M. Fejer, *Pulse Compression during second-harmonic generation in aperiodic quasi-phasematched gratings*, accepted *Opt. Lett.* **22**, 865, 1997.
107. G. Imeshev, M. Proctor and M. M. Fejer, *Lateral Patterning of Nonlinear Frequency Conversion with Radially Varying Quasi-phasematched Gratings*, to be present at the CLEO 97 Conference, Baltimore, MD May 18–23 (1997).
108. L. E. Myers, G. D. Miller, R. C. Eckardt, M. M. Fejer and R. L. Byer, *Quasi-phasematched 1.064 μm -pumped optical parametric oscillator in bulk periodically poled LiNbO_3* , *Opt. Lett.* **20**, 52 (1995).
109. J. J. Zahowsky, *Periodically poled lithium niobate optical parametric amplifiers pumped by high-power passively Q-switched microchip laser*, *Opt. Lett.* **22**, 169 (1997).
110. W. R. Bosenberg, A. Drobshoff, D. C. Gerstenberger, L. E. Myers, R. C. Eckardt, M. M. Fejer and R. L. Byer, *Long Pulse Optical Parametric Oscillator based on Bulk Periodically Poled LiNbO_3* , published in the *OSA Proceeding on Advanced Solid State Laser*, **24**, 42 (1995).
111. L. E. Myers, R. C. Eckardt, M. M. Fejer, R. L. Byer, J. W. Pierce and R. G. Beausoleil, *CW Diode-Pumped Optical Parametric Oscillator in Bulk Periodically Poled LiNbO_3* , published in *OSA Proceedings on Advanced Solid State Lasers*, **24**, 57 (1995); L. E. Myers, R. C. Eckardt, M. M. Fejer, R. L. Byer and J. W. Pierce, *CW diode-pumped optical parametric oscillator in bulk periodically poled LiNbO_3* , *Electr. Letts.* **31**, 1869 (1995).
112. L. Goldberg, W. Burns and R. McElhanon, *Widely tunable difference frequency generation in QPM- LiNbO_3* , *Conf. on Lasers and Electrooptics*, 1995 postdeadline paper CPD49; L. Goldberg, W. Burns and R. McElhanon, *Difference-frequency generation of tunable mid-infrared radiation in bulk periodically poled LiNbO_3* , *Opt. Lett.* **20**, 1280 (1995).
113. S. Sanders, R. J. Lang, L. E. Myers, M. M. Fejer and R. L. Byer, *Broadly tunable mid-IR radiation source based on difference frequency mixing of high power wavelength tunable laser diodes in bulk periodically poled LiNbO_3* , *Electr. Letts.* **32**, 218 (1996).
114. A. Balakrishnan, S. Sanders, S. DeMars, J. Webjorn, D. W. Nam, R. J. Lang, D. G. Meyhuys, R. G. Waarts and D. F. Welch, *Broadly tunable laser-diode-based mid-infrared source with up to 31 μW of power at 4.3 μm wavelength*, *Opt. Lett.* **21**, 952 (1996).
115. K. P. Petrov, L. Goldberg, W. K. Burns, R. F. Curl and F. K. Tittle, *Detection of CO in air by diode-pumped 4.6 μm difference-frequency generation in quasi-phasematched LiNbO_3* , *Opt. Lett.* **21**, 86 (1996).
116. Y.-L. Lu, Y.-Q. Lu, C.-C. Xue and N.-B. Ming, *Growth of Nd^{3+} -doped LiNbO_3 optical superlattice crystals and its potential applications in self-frequency doubling*, *Appl. Phys. Lett.* **68**, 1467 (1996); Y.-L. Lu, Y.-Q. Lu, X.-F. Cheng, G.-P. Luo, C.-C. Xue and N.-B. Ming, *Formation mechanism for ferroelectric domain structures in a LiNbO_3 optical superlattice*, *Appl. Phys. Lett.* **68**, 2642 (1996); Y.-L. Lu, X.-F. Cheng, C.-C. Xue and N.-B. Ming, *Growth of optical superlattice LiNbO_3 with different modulating periods and its applications in second-harmonic generation*, *Appl. Phys. Lett.* **68**, 2781 (1996).
117. Y.-L. Lu, J.-J. Zheng, C.-C. Xue, X.-F. Cheng and N.-B. Ming, *Efficient continuous wave blue light generation in optical superlattice LiNbO_3 by direct frequency doubling a 978 nm InGaAs diode laser*, *Appl. Phys. Lett.* **69**, 1660 (1996).
118. Y.-Q. Lu, Y.-L. Lu, C.-C. Xue, J.-J. Zheng, X.-F. Chen, G.-P. Luo, N.-B. Ming, D.-H. Feng and X.-L. Zhang, *Femtosecond violet light generation by quasi-phasematched frequency doubling in optical superlattice LiNbO_3* , *Appl. Phys. Lett.* **69**, 3155 (1996).

119. W. S. Hu, Z. G. Liu, Y-Q. Lu, S. N. Zhu and D. Feng, *Pulsed-laser deposition and optical properties of completely (001) textured optical waveguiding LiNbO₃ films upon SiO₂/Si substrates*, *Opt. Lett.* **21**, 946 (1996).
120. C. Baron, H. Cheng and M. C. Gupta, *Domain inversion in LiTaO₃ and LiNbO₃ by electric field application on chemically patterned crystals*, *Appl. Phys. Lett.* **68**, 481 (1996).
121. K. Mizuuchi and K. Yamamoto, *Generation of 340 nm light by frequency doubling of a laser in bulk periodically poled LiTaO₃*, *Opt. Lett.* **21**, 107 (1996).
122. A. Harada and Y. Nihei, *Bulk periodically poled MgO-LiNbO₃ by corona discharge method*, *Appl. Phys. Lett.* **69**, 2629 (1996).
123. Y. Kitaoka, K. Mizuuchi, K. Yamamoto, M. Kato and T. Sasaki, *Intracavity second-harmonic generation with a periodically domain-inverted LiTaO₃ device*, *Opt. Lett.* **21**, 1972 (1996).
124. W. P. Risk and S. D. Lau, *Periodic electric field poling of KTiOPO₄ using chemical patterning*, *Appl. Phys. Lett.* **69**, 3999 (1996).
125. M. H. Chou, M. A. Arbore and M. M. Fejer, *Adiabatically tapered periodic segmentation of channel waveguides for mode-size transformation and fundamental mode excitation*, *Opt. Lett.* **21**, 794 (1996).
126. M. Taya, M. C. Bashaw and M. M. Fejer, *Photorefractive effects in periodically poled ferroelectrics*, *Opt. Lett.* **21**, 857 (1996).
127. V. Pruneri, S. D. Butterworth and D. C. Hanna, *Highly efficient green-light generation by quasi-phasematched frequency doubling of picosecond pulses from an amplified mode-locked Nd:YLF laser*, *Opt. Lett.* **21**, 390 (1996).
128. V. Pruneri, S. D. Butterworth and D. C. Hanna, *Low-threshold picosecond optical parametric oscillation in quasi-phasematched lithium niobate*, *Appl. Phys. Lett.* **69**, 1029 (1996).
129. S. D. Butterworth, V. Pruneri and D. C. Hanna, *Optical parametric oscillation in periodically poled lithium niobate based on continuous wave synchronous pumping at 1.047 μm* , *Opt. Lett.* **21**, 1345 (1996).
130. M. A. Arbore, M. M. Fejer, M. E. Fermann, A. Hariharan, A. Galvanauskas and D. Harter, *Frequency doubling of femtosecond erbium-fiber soliton lasers in periodically poled lithium niobate*, *Opt. Lett.* **22**, 13 (1997).
131. A. Galvanauskas, M. A. Arbore, M. M. Fejer, M. E. Fermann and D. Harter, *Fiber-laser-based femtosecond parametric generator in bulk periodically poled LiNbO₃*, *Opt. Lett.* **22**, 105 (1997).
132. G. D. Miller, R. G. Batchko, M. M. Fejer and R. L. Byer, *Visible quasi-phasematched harmonic generation by electric-field-poled lithium niobate*, *SPIE 2700*, 34 (1996).
133. L. E. Myers, W. R. Bosenberg, J. I. Alexander, M. A. Arbore, M. M. Fejer and R. L. Byer, *CW Singly-Resonant Optical Parametric Oscillators Based on 1.046 μm Pumped Periodically Poled LiNbO₃*, *OSA TOPS Advanced Solid State Lasers*, **1**, 35 (1996).
134. W. R. Bosenberg, A. Drobshoff, J. I. Alexander, L. E. Myers and R. L. Byer, *Continuous wave singly-resonant optical parametric oscillator based on periodically poled LiNbO₃*, *Opt. Lett.* **21**, 713 (1996).
135. W. R. Bosenberg, A. Drobshoff, J. I. Alexander, L. E. Myers and R. L. Byer, *93% pump depletion, 3.5 W continuous-wave, singly-resonant optical parametric oscillator*, *Opt. Lett.* **21**, 1336 (1996).
136. L. E. Myers, R. C. Eckardt, M. M. Fejer and R. L. Byer, *Multigrating quasi-phasematched optical parametric oscillator in periodically poled LiNbO₃*, *Opt. Lett.* **21**, 591 (1996).

137. G. D. Miller, R. G. Batchko, W. M. Tulloch, D. R. Weise, M. M. Fejer and R. L. Byer, *42% efficient single-pass second-harmonic generation of continuous-wave Nd:YAG laser output in 5.3 cm length periodically-poled lithium niobate*, presented at the Advanced Solid State Laser Conference, January 27-29, 1997, Orlando, FL (to be published).
138. R. G. Batchko, D. R. Weise, T. Plettner, G. D. Miller, M. M. Fejer and R. L. Byer, *532 nm-Pumped Continuous-Wave Singly Resonant Optical Parametric Oscillator Based on Periodically Poled Lithium Niobate*, presented at the Advanced Solid State Laser Conference, January 27-29, 1997, Orlando, FL.
139. A photograph of the 532 nm pumped cw SRO appeared on the cover of the May 1997 edition of *Laser Focus World*.
140. M. E. Anderson, M. Beck, M. G. Raymer and J. D. Bierlein, *Opt. Lett.* **20**, 620 (1995).
141. D. K. Serkland, M. M. Fejer, R. L. Byer and Y. Yamamoto, *Squeezing in a quasi-phasematched LiNbO₃ waveguide*, *Opt. Lett.* **20**, 1649 (1995).
142. D. J. Lovering, J. A. Levenson, P. Vidakovic, J. Webjorn and P. St. J. Russell, *Noiseless optical amplification in quasi-phasematched bulk lithium niobate*, *Opt. Lett.* **21**, 1439 (1996).
143. G. I. Stegeman, E. M. Wright, N. Finlayson, R. Zanoni and C. T. Seaton, *J. Lightwave Technol.* **6**, 953 (1988).
144. M. Asobe, I. Yokohama, H. Itoh and T. Kaino, *All-optical switching by use of cascading of phasematched sum-frequency-generation and difference-frequency-generation processes in periodically poled LiNbO₃*, *Opt. Lett.* **22**, 274 (1997).
145. P. Vidakovic, D. J. Lovering, J. A. Levenson, J. Webjorn and P. St. J. Russell, *Large nonlinear phase shift owing to cascade $\chi^{(2)}$ in quasi-phasematched bulk LiNbO₃*, *Opt. Lett.* **22**, 277 (1997).
146. Y. Chui, D. D. Stancil, T. E. Schlesinger and W. P. Risk, *Electro-optic beam scanner in KTiOPO₄*, *Appl. Phys. Lett.* **69**, 3134 (1996).
147. M. Yamada, M. Saitoh and H. Ooki, *Electric-field induced cylindrical lens, switching and deflection devices composed on the inverted domains of LiNbO₃ crystals*, *Appl. Phys. Lett.* **69**, 3659 (1996).
148. M. M. Fejer, S. J. B. Yoo and R. L. Byer, *Observation of Extremely Large Quadratic Susceptibility at 9.6-10.8 μm in Electric-Field Biased AlGaAs Quantum Wells*, *Phys. Rev. Letts.* **62**, (1989).
149. H. C. Chui, G. L. Woods, M. M. Fejer, E. L. Martinet and S. J. Harris, Jr. *Tunable mid-infrared generation by difference frequency mixing of diode laser wavelength in intersubband InGaAs/AlAs quantum wells*, *Appl. Phys. Lett.* **66**, 265 (1995).
150. M. J. Angell, R. M. Emerson, J. L. Hoyt, J. F. Gibbons, L. A. Eyres, M. L. Bortz and M. M. Fejer, *Growth of alternating (100)/(111) oriented II-VI regions for quasi-phasematched nonlinear optical on GaAs substrates*, *Appl. Phys. Lett.* **64**, 3107 (1994).
151. S. J. B. Yoo, C. Caneau, R. Bhat, M. A. Koza, A. Rajhel and Neo Antoniadis, *Wave-length conversion by difference frequency generation in AlGaAs waveguides with periodic domain inversion achieved by wafer bonding*, *Appl. Phys. Lett.* **68**, 2609 (1996).
152. L. Gordan, G. L. Woods, R. C. Eckardt, R. R. Route, R. S. Feigelson, M. M. Fejer and R. L. Byer, *Diffusion-bonded stack GaAs for quasi-phasematched second-harmonic generation of a carbon dioxide laser*, *Electr. Letts.* **29**, 1942 (1993).